# The serine-glycine-one-carbon metabolic network orchestrates changes in nitrogen and sulfur metabolism and shapes plant development

Sara Rosa-Téllez , 1,2,\*,† Andrea Alcántara-Enguídanos , 1,2,† Federico Martínez-Seidel , 3 Ruben Casatejada-Anchel , 1,2 Sompop Saeheng , 4,† Clayton L. Bailes , 4 Alexander Erban , 5 David Barbosa-Medeiros , 3,5 Paula Alepúz , 1,5 José Tomás Matus , 6 Joachim Kopka , 3 Jesús Muñoz-Bertomeu , 2 Stephan Krueger , 7 Sanja Roje , 4 Alisdair R. Fernie , and Roc Ros , 4 Alisdair R. Fernie

- 1 Institut de Biotecnologia i Biomedicina (BIOTECMED), Universitat de València, 46100 Burjassot, Spain
- 2 Departament de Biologia Vegetal, Facultat de Farmàcia, Universitat de València, 46100 Burjassot, Spain
- 3 Max Planck Institute of Molecular Plant Physiology, 14476 Potsdam-Golm, Germany
- 4 Institute of Biological Chemistry, Washington State University, Pullman, WA 99164, USA
- 5 Departament de Bioquímica y Biologia Molecular, Facultat de Biologia, Universitat de València, 46100 Burjassot, Spain
- 6 Institute for Integrative Systems Biology, I<sup>2</sup>SysBio, Universitat de València—CSIC, 46908 Paterna, Spain
- 7 Institute for Plant Sciences, University of Cologne, Zülpicherstraße 47b, 50674 Cologne, Germany

The author responsible for distribution of materials integral to the findings presented in this article in accordance with the policy described in the Instructions for Authors (https://academic.oup.com/plcell/pages/General-Instructions) is: Roc Ros Palau (roc.ros@uv.es).

#### **Abstract**

L-serine (Ser) and L-glycine (Gly) are critically important for the overall functioning of primary metabolism. We investigated the interaction of the phosphorylated pathway of Ser biosynthesis (PPSB) with the photorespiration-associated glycolate pathway of Ser biosynthesis (GPSB) using *Arabidopsis thaliana* PPSB-deficient lines, GPSB-deficient mutants, and crosses of PPSB with GPSB mutants. PPSB-deficient lines mainly showed retarded primary root growth. Mutation of the photorespiratory enzyme Ser-hydroxymethyltransferase 1 (SHMT1) in a PPSB-deficient background resumed primary root growth and induced a change in the plant metabolic pattern between roots and shoots. Grafting experiments demonstrated that metabolic changes in shoots were responsible for the changes in double mutant development. PPSB disruption led to a reduction in nitrogen (N) and sulfur (S) contents in shoots and a general transcriptional response to nutrient deficiency. Disruption of SHMT1 boosted the Gly flux out of the photorespiratory cycle, which increased the levels of the one-carbon (1C) metabolite 5,10-methylene-tetrahydrofolate and S-adenosylmethionine. Furthermore, disrupting SHMT1 reverted the transcriptional response to N and S deprivation and increased N and S contents in shoots of PPSB-deficient lines. Our work provides genetic evidence of the biological relevance of the Ser–Gly–1C metabolic network in N and S metabolism and in interorgan metabolic homeostasis.

<sup>\*</sup>Author for correspondence: roc.ros@uv.es (R.R.), sara.rosa@uv.es (S.R.-T.)

<sup>&</sup>lt;sup>†</sup>These authors contributed equally and are cofirst authors.

<sup>&</sup>lt;sup>‡</sup>Present address: Division of Health and Applied Sciences, Faculty of Science, Prince of Songkla University, Hatyai, Songkhla, 90110, Thailand.

<sup>§</sup>Present address: Syngenta Seeds Ltda, Caixa Postal 585, 38407-049, Uberlândia, MG, Brazil.

These authors jointly supervised this work and are cosenior authors.

#### IN A NUTSHELL

**Background:** Photorespiration, in which Rubisco adds oxygen to RuBP instead of adding carbon dioxide, thus lowering photosynthetic output, is a key metabolic pathway that will be affected by rising temperatures and increasing atmospheric CO<sub>2</sub> levels. For a long time, this pathway has been considered a wasteful process that consumes energy in the form of adenosine triphosphate (ATP) and reducing power. It also leads to the futile loss of carbon units as CO<sub>2</sub>, consequently constraining plant growth and yield. However, recent studies suggest that future climate conditions, which may reduce photorespiratory activity, may also enhance plant biomass albeit at the cost of decreased crop nutritional value.

Question: Should we consider photorespiration only as a loss-inducing process?

**Findings:** Our research reveals the crucial role of glycine flux regulation by photorespiration in maintaining nitrogen, carbon, and sulfur balance in plants. Redirecting glycine flux out of the photorespiratory pathway has a positive effect on plant nitrogen and sulfur levels. Our findings shed light on the molecular mechanisms through which reduced photorespiration adversely affects crop nutritional value. In mammals, the serine–glycine–one-carbon metabolic network functions as a central integrator of nutrient status. We propose a similar role for this network in plants.

**Next steps:** Our findings open new avenues for enhancing crop nutritional quality under future climate change conditions, particularly with regard to nitrogen content, an essential component of proteins and nucleic acids. Validating the feasibility of this biotechnological approach will require additional experiments conducted in natural environments across different species and under varying conditions of temperature, light, and CO<sub>2</sub>.

#### Introduction

The L-serine (Ser)-L-glycine (Gly)-one carbon (1C) metabolic network is required for the biosynthesis of nucleotides, proteins, and lipids. This network also drives the methyltransferase reactions governing epigenetic regulation and the supply of almost all methylated metabolites (Fig. 1). In mammals, the Ser-Gly-1C network supports the uninhibited proliferation of cancer cells and is associated with tumor progression (Locasale et al. 2011; Possemato et al. 2011; Pacold et al. 2016; Ducker and Rabinowitz 2017; Reina-Campos et al. 2019; Geeraerts et al. 2021). As a major 1C donor, Ser plays a crucial role in the regulation and function of Ser-Gly-1C metabolism in mammals (Locasale 2013; Yang and Vousden 2016) where it is mainly synthesized by the socalled phosphorylated pathway of Ser biosynthesis (PPSB) located in the cytosol. Ser biosynthesis in plants is much more complex and consists of 3 pathways. The first pathway, the glycolate pathway of Ser biosynthesis (GPSB), is associated with photorespiration and operates in mitochondria. In addition, there are 2 alternative nonrelated photorespiratory pathways: the PPSB (located in plastids) and the glycerate pathway (in peroxisomes).

In plants, the PPSB was long considered to be a minor pathway. However, functional characterization of PPSB genes demonstrated that this pathway is essential for male gametophyte and embryo development and for root growth (Benstein et al. 2013; Cascales-Miñana et al. 2013; Toujani et al. 2013; Wulfert and Krueger 2018). Cell proliferation and elongation analysis revealed that PPSB is indispensable for normal meristem development (Zimmermann et al. 2021). The plant PPSB defines a branch point for the 3-phosphoglycerate (3-PGA) produced in plastidial glycolysis and comprises 3 sequential reactions catalyzed by 3-PGA

dehydrogenase (PGDH), 3-phosphoSer aminotransferase (PSAT), and 3-phosphoSer phosphatase (PSP; Fig. 1) (Ho and Saito 2001). In *Arabidopsis thaliana* (Arabidopsis), 3 genes encode PGDHs (*PGDH1*, *PGDH2*, and *PGDH3*), 2 encode PSAT (*PSAT1* and *PSAT2*), and one encodes PSP (*PSP1*) (Ros et al. 2014).

The GPSB has been regarded as the plant's most important Ser biosynthesis pathway due to the high flux borne by photorespiration (Tolbert 1997; Douce et al. 2001). The GPSB is the result of the oxygenase activity of Rubisco, which depends on the CO<sub>2</sub>/O<sub>2</sub> ratio in the atmosphere (Ogren and Bowes 1971; Ogren 2003). This  $CO_2/O_2$  ratio determines whether Rubisco acts as a carboxylase, producing 2 molecules of 3-PGA in the Calvin-Benson cycle, or as an oxygenase, producing one molecule of 3-PGA and one of the potent enzyme inhibitor 2-phosphoglycolate (2-PG). This 2-PG is recycled to 3-PGA through a series of enzymatic reactions of the photorespiratory cycle that takes place in the chloroplasts, peroxisomes, and mitochondria (Fig. 1). In this cycle, 2 molecules of 2-PG (2C each) are needed to recover one molecule of 3-PGA (3C), and one of the 4C atoms is released as CO<sub>2</sub>. In addition, the photorespiratory cycle loses reduced nitrogen (N) as NH<sub>3.</sub> which has to be reassimilated in a high energy-consuming pathway called the photorespiratory nitrogen cycle (Fig. 1). For this reason, photorespiration was long considered to be a futile cycle with the largest energy losses in plants (Bauwe et al. 2010; Peterhansel et al. 2010).

However, photorespiration integrates and participates in other pathways (Shi and Bloom 2021). First, photorespiration contributes to the pools of Gly and Ser. The photorespiratory Gly-decarboxylase complex (GDC) and Ser-hydroxymethyl-transferase 1 (SHMT1) in the mitochondria of photosynthetic cells convert 2 Gly molecules into one Ser molecule (Fig. 1).

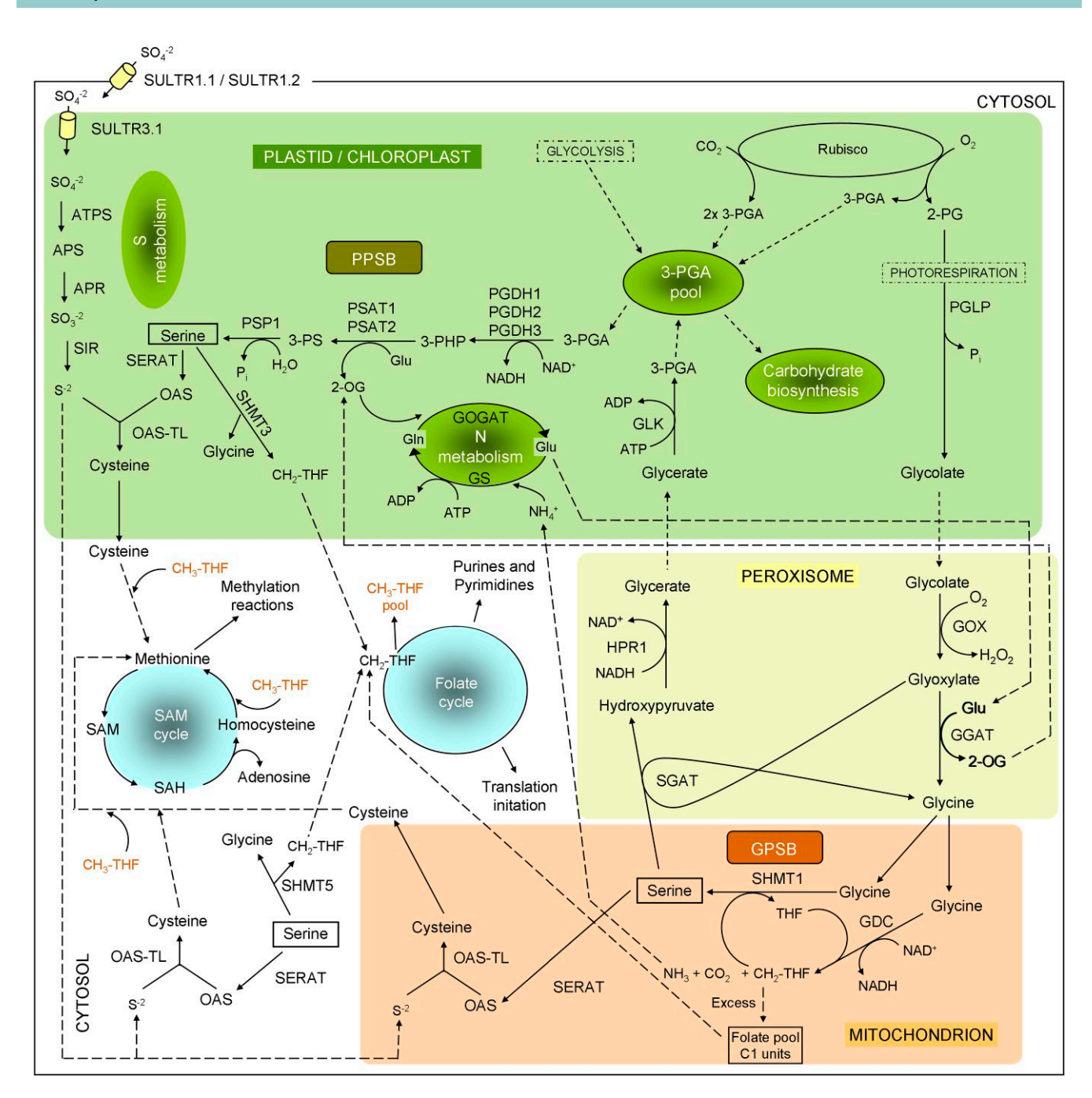


**Figure 1.** Schematic representation of the phosphorylated pathway (PSPB) and glycolate pathway (GPSB) of serine biosynthesis and putative interactions with other primary metabolic pathways. Enzymes and transporters: APR, APS reductase; ATPS, ATP sulfurylase; GDC, glycine-decarboxylase complex; GGAT, glutamate-glyoxylate aminotransferase; GLK, glycerate kinase; GOGAT, glutamine-oxoglutarate aminotransferase; GOX, glycolate oxidase; GS, glutamine-synthetase; HPR, hydroxypyruvate reductase; OAS-TL, O-acetylserine-(thiol)-lyase; PGDH, 3-phosphoglycerate dehydrogenase; PGLP, 2-phosphoglycolate phosphatase; PSAT, 3-phosphoserine aminotransferase; PSP1, 3-phosphoserine phosphatase; SERAT, serine-acetyltransferase; SHMT, serine-hydroxymethyltransferase; SIR, sulfite reductase. Metabolites: 3-PHP, 3-phosphohydroxypyruvate; 3-PS, 3-phosphoserine; CH<sub>3</sub>-THF, 5-methyl-THF; APS, adenosine 5'-phosphosulfate; C1, one-carbon metabolite; CH<sub>2</sub>-THF, 5,10-methylene-THF; Gln, glutamine; Glu, glutamate; OAS, O-acetylserine; SAH, S-adenosylhomocysteine.

One Gly molecule is cleaved by GDC releasing  $CO_2$  and  $NH_3$ . The remaining methylene C of Gly is transferred to tetrahydrofolate (THF) to form 5,10-methylene-THF ( $CH_2$ -THF) and NADH, which react with a second Gly to form Ser in a reaction catalyzed by SHMT (Fig. 1). The GDC complex activity

exceeds that of SHMT1 in vitro (Rebeille et al. 1994; Douce et al. 2001), which led to the assumption that CH<sub>2</sub>-THF accumulates in the mitochondria relative to THF. Ser produced by SHMT in mitochondria and that synthesized by PPSB in plastids can be transported to the cytosol, where they can also be

used to produce 1C-units by the reverse reaction catalyzed by the cytosolic SHMTs (Mouillon et al. 1999; Engel et al. 2007). Cytosolic 1C units are employed for methionine (Met) biosynthesis, which is then incorporated into proteins or used for the production of the universal methyl donor S-AdenosylMet (SAM) (Fig. 1). Moreover, 1C units are also utilized to synthesize purines and pyrimidines (Rébeillé et al. 2006; Hanson and Gregory 2011; Gorelova et al. 2017; Mohanta et al. 2019). Although the SHMT1/GDC activity has been considered to be the major source of 1C units for plants (Bauwe and Kolukisaoglu 2003), genetic and metabolic evidence about the contribution of these photorespiratory reactions to the folate and SAM cycles is missing. Moreover, the contribution of the PPSB-derived Ser to 1C-folate metabolism is unknown.

As the oxygenase activity of Rubisco depends on the  $CO_2$ / O<sub>2</sub> ratio, the supply of Ser-Gly-1C by GPSB to plants will be influenced by increases in the atmospheric CO<sub>2</sub> concentration resulting from anthropogenic activity. Furthermore, as Ser is recycled by photorespiration to 3-PGA (Fig. 1), the absolute contribution of GPSB to the supply of Ser for plant metabolism and development remains controversial. Modeling and isotopic labeling studies estimated that under ambient CO<sub>2</sub> (aCO<sub>2</sub>) concentrations, a substantial fraction of the photorespiratory Gly and Ser is not recycled back to 3-PGA, but it is used in other metabolic pathways as precursors of molecules required for growth, such as nucleotides or proteins (Abadie et al. 2016; Busch et al. 2018; Fu et al. 2023). However, under elevated CO<sub>2</sub> (eCO<sub>2</sub>) growth conditions, when GPSB activity is restricted, increase in Arabidopsis biomass provided that PPSB remains functional, indicating that the PPSB-derived Ser contributes more to plant growth than the GPSB-derived Ser (Zimmermann et al. 2021). These findings highlight the complexity of the interaction of both pathways and indicate that their contribution to other metabolic networks is not completely understood. In this regard, it has been described that photorespiration and PPSB may contribute to N and sulfur (S) assimilation (Rachmilevitch et al. 2004; Bloom et al. 2010; Abadie et al. 2016; Busch et al. 2018; Samuilov et al. 2018a, 2018b; Abadie and Tcherkez 2019; Anoman et al. 2019; Zimmermann et al. 2021). The role of PPSB and GPSB in these metabolic networks may be especially important for crops in a scenario in which the continuous increase in atmospheric CO<sub>2</sub> concentrations may reduce photorespiration and thus limit crop nutritional quality (Bloom et al. 2010; Bloom et al. 2012, 2014; Jauregui et al. 2015, 2016; Walker et al. 2016). Nonetheless, the connections between PPSB and GPSB with N and S metabolism and especially their biological relevance in terms of their contribution to overall plant nutrient status and development remain unclear.

In this study, we aimed to clarify the relative contributions of both PPSB and GPSB to Ser-Gly-1C biosynthesis and to gain insight into how they interact with N, S, and C metabolism. Previous attempts to block both PPSB and photorespiration have been unsuccessful. Therefore, studies were

conducted using PPSB-deficient lines under conditions that favored or disfavored photorespiration (Zimmermann et al. 2021). Here, we used a combination of PPSB-deficient and SHMT1-deficient lines. In this way, we could bypass the reaction producing Ser in the GPSB without short-circuiting the photorespiratory cycle. We show that the regulation of Ser/Gly flux by PPSB and GPSB affects N, C, and S homeostasis. Our work provides genetic evidence of the biological significance of the Ser–Gly–1C metabolic network in N and S metabolism and in organ developmental patterns in Arabidopsis. Our study unravels essential steps of photorespiration, which might be used to develop new crops with higher nutritional value.

#### Results

Interactions of PPSB and GPSB modify the developmental pattern of aerial parts/roots of plants Figure 2 shows that both PGDH1- and PSP1-deficient Arabidopsis lines (c-psp1 and c-pgdh1), with low background levels of PGDH1 and PSP1, respectively (Cascales-Miñana et al. 2013; Casatejada-Anchel et al. 2021), displayed more dramatic growth phenotypes under eCO2, where GPSB activity is reduced, than under aCO<sub>2</sub> (Fig. 2, A and B), which corroborates the notion that PPSB and GPSB cooperate in supplying Ser for plant growth (Zimmermann et al. 2021). Accordingly, PGDH1 and PGDH2, the 2 main PGDH family genes (Casatejada-Anchel et al. 2021), were induced in shoots of wild-type (WT) plants under eCO<sub>2</sub> growth conditions (Fig. 2C). Under these conditions, PGDH1 and especially PGDH2 were also induced in c-psp1 lines, as well as PGDH2 in c-pghd1 lines, suggesting the general upregulation of the PPSB in response to PSP1 or PGDH1 inactivation (Fig. 2D). However, SHMT1 was repressed in PPSB-deficient lines. Besides, neither PGDH1 nor PGDH2 was induced in the roots of a mutant of SHMT1 (shmt1.2, henceforth shmt1) in which PGDH2 was even repressed. These results indicate that the interactions between the 2 Ser biosynthetic pathways are complex.

In the first attempt to complement the growth phenotype of PPSB-deficient lines, we blocked photorespiration at the level of serine-glyoxylate aminotransferase (SGAT), which is the peroxisomal enzyme that converts Ser into hydroxypyruvate in the photorespiratory cycle (Fig. 1). SGAT could be a key point in the control of the Ser pool since it was shown that sgat mutants have increased Ser levels and that SGAT overexpression reduces Ser levels (Somerville and Ogren 1980; Modde et al. 2017). In our experimental conditions, the sgat1 mutants accumulated more Ser than WT when grown under aCO<sub>2</sub> and eCO<sub>2</sub> conditions (Supplemental Fig. S1). However, the sgat1 mutation in the PGDH-silenced lines was lethal.

The finding that SHMT1 was repressed in PPSB-deficient lines led us to introduce the shmt1 mutation into the PPSB-deficient mutant background (shmt1 c-psp1 and

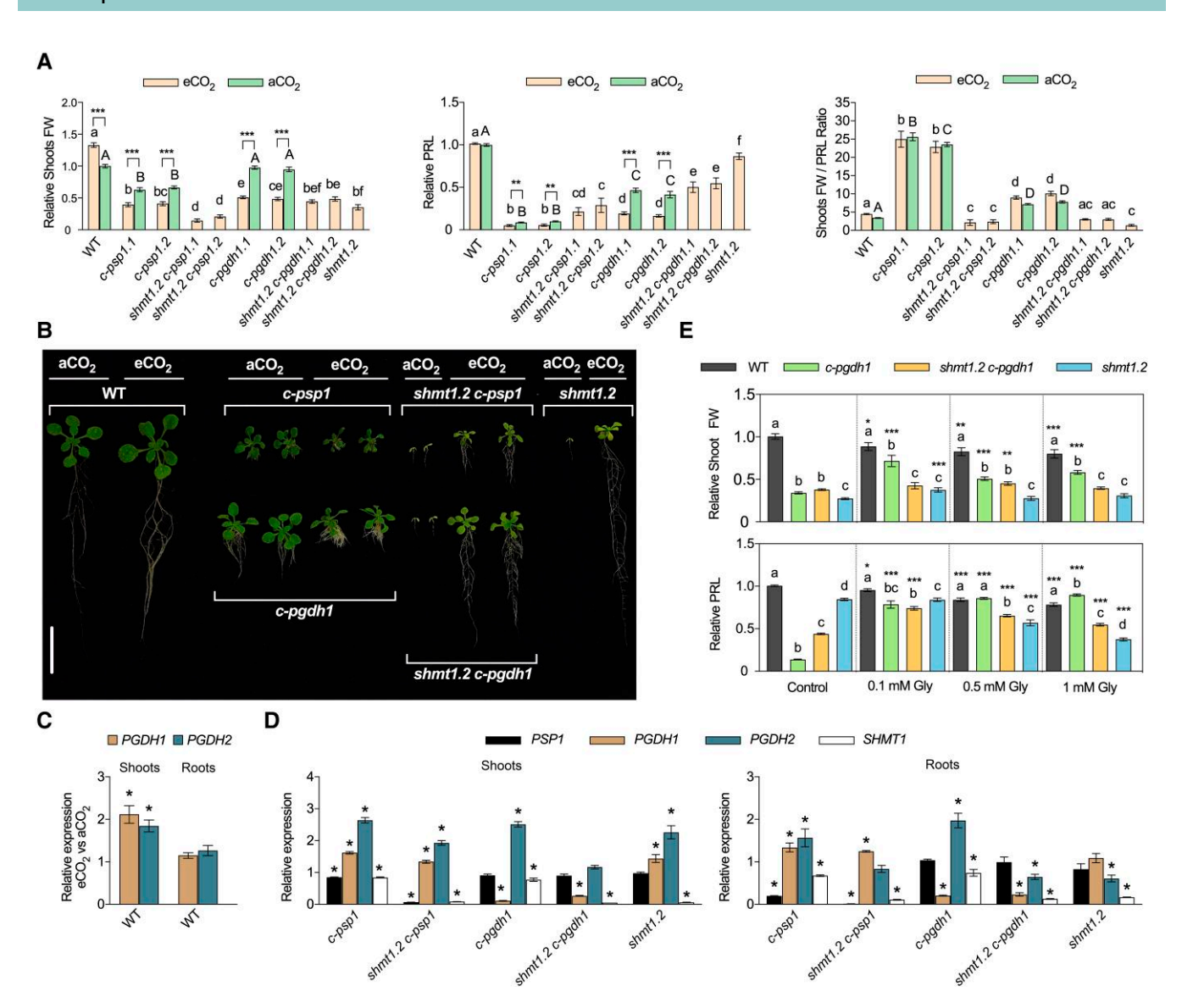


Figure 2. Characterization of PPSB-deficient (*c-psp1* and *c-pgdh1*) and SHMT1-deficient (*shmt1.2*, *shmt1.2 c-psp1*, and *shmt1.2 c-pgdh1*) lines. A) Relative shoot fresh weight (FW), primary root length (PRL), and shoot FW/PRL ratio of different lines grown under aCO<sub>2</sub> or eCO<sub>2</sub> conditions compared to WT plants. B) Photograph of representative individuals of each line grown under aCO<sub>2</sub> or eCO<sub>2</sub> conditions. C) *PGDH1* and *PGDH2* expression in shoots and roots of WT lines under eCO<sub>2</sub> compared with aCO<sub>2</sub> conditions. D) *PSP1*, *PGDH1*, *PGDH2*, and *SHMT1* expression in different lines grown under eCO<sub>2</sub> compared with WT. E) Relative shoot FW and PRL of different lines grown under eCO<sub>2</sub> supplemented with Gly. In A) and E) (mean  $\pm$  se,  $n \ge 7$ ; data represent the mean of at least 10 plants), values are normalized to the mean calculated for the WT under aCO<sub>2</sub> A) or eCO<sub>2</sub> conditions E); different letters indicate significant differences between lines (P < 0.05) under the same growth conditions; significant differences between growth conditions, as determined by Student's *t*-test, are denoted by \* (P < 0.05), \*\*\* (P < 0.01), or \*\*\*\* (P < 0.001). C and D) Values (mean  $\pm$  se;  $n \ge 4$  independent biological replicates of pools of 40 plants) are normalized to the gene expression under aCO<sub>2</sub> conditions C) or to the WT background D); significant differences between aCO<sub>2</sub> and eCO<sub>2</sub> gene expression C) or between mutants and WT D), as determined by Student's *t*-test, are denoted by \* (P < 0.05). Scale bar = 2 cm B).

shmt1 c-pgdh1). In contrast to PPSB-deficient lines, PGDH2 expression was no longer induced in shmt1 c-pgdh1 shoots and shmt1 c-psp1 roots, while it was even repressed in the roots of shmt1 c-pgdh1 lines, indicating a general downregulation of the PPSB pathway in these mutant backgrounds. We characterized single and double mutants under eCO<sub>2</sub> and aCO<sub>2</sub> whenever possible. In single mutants, the PPSB deficiency (c-psp1 and c-pgdh1) mainly affected primary root growth, while the SHMT1 mutation mostly affected shoot

growth (Fig. 2, A and B). For instance, under aCO<sub>2</sub>, the shoot fresh weight of the *c-pgdh1* lines was unchanged, while the primary root length was reduced by more than 50% compared with WT. Under eCO<sub>2</sub>, the same growth trend, albeit more exacerbated, was observed for both *c-psp1* and *c-pgdh1*. Under these conditions, *shmt1* showed a 65% reduction in shoot biomass, while the primary root length was only reduced by 13%. The *shmt1* mutation in PPSB-deficient lines maintained (*shmt1 c-pgdh1*) or reduced (*shmt1 c-psp1*) shoot

growth versus their respective PPSB-deficient lines (*c-pgdh1* or *c-psp1*). Interestingly, the primary root length recovered in the double mutants between 2.6-fold and 5.2-fold longer than in the respective PPSB-deficient lines. These results indicate a change in the shoot/root developmental pattern in the double mutants, as quantified by the shoot fresh weight/primary root length ratio (Fig. 2A). This ratio was always higher in *c-pgdh1* than in the *shmt1 c-pgdh1* lines, while the lowest shoot fresh weight/primary root length ratio was found in the *shmt1* line (Fig. 2A). Altogether, phenotypic characterization and expression data suggest that Ser homeostasis might be modified in the double-mutant lines.

### Disrupting SHMT1 profoundly alters N and C metabolism in PPSB-deficient lines

To investigate the effect of disrupting SHMT1 on central metabolism, we measured the major C and N metabolites in plants grown under eCO<sub>2</sub> conditions under which SHMT1-deficient lines are viable (Fig. 3). Glycolate measurements in shoots, a key metabolite at the beginning of the photorespiratory pathway and the product of the metabolization of toxic 2-PG, showed that its content in shmt1 c-pgdh1 and shmt1 was not higher than in WT or c-pgdh1 lines (Supplemental Fig. S2). This result suggests that metabolites upstream of glycolate in the photorespiratory pathway, such as 2-PG, did not accumulate more in mutants with a shmt1 background than in other lines under the low photorespiratory growth conditions used in this work (eCO2 and 100  $\mu$ mol m<sup>-2</sup> s<sup>-1</sup> light intensity). However, principal component analysis (PCA) of metabolites revealed clear differences between lines (Fig. 3, A and D). The metabolite whose levels differed most strongly between lines in shoots and roots was the amino acid Gly. Like the shmt1 parental lines, double shmt1 PPSB-deficient lines showed a dramatic increase in Gly levels in shoots and roots compared with the other lines. These lines also displayed higher Ser levels than their respective single PPSB-deficient lines, although the changes were not as dramatic as for Gly. In fact, the common pattern of all SHMT1-deficient lines (shmt1, shmt1 c-psp1, and shmt1 c-pgdh1) had a much higher shoot Gly/Ser ratio than WT or PPSB-deficient lines, suggesting that Gly metabolism was more strongly altered than the Ser metabolism in these lines (Fig. 3B). Therefore, diverting the photorespiratory flux before Ser biosynthesis by SHMT1 changes the Gly/Ser ratio in shoots. Gly-feeding experiments confirmed that this amino acid can complement the root growth phenotypes of PPSB-deficient mutants (Fig. 2E). However, externally supplied Gly differently affected the root growth response, depending on the mutant background and the concentration. Thus, Gly concentrations of 0.5 mm or higher clearly inhibited primary root growth compared with controls without Gly supplementation in WT and shmt1 plants, especially the latter. However, these Gly concentrations still had a positive effect on the primary root growth of c-pgdh1 lines. These results indicate that greater levels of external Gly are required in PPSB-deficient lines.

Other major metabolite changes between lines were the accumulation of transport amino acids, such as glutamate (Glu), glutamine (Gln), and aspartate (Asp), and Asp-derived amino acids, such asparagine (Asn) and Met in shoots of SHMT1-deficient lines compared with WT and PPSBdeficient lines (Fig. 3, A and C). By contrast, the levels of soluble sugars such as glucose and fructose were reduced in these lines: in roots, Glu, Gln, Asp, and Asn no longer accumulated in SHMT1-deficient versus PPSB-deficient lines (Fig. 3F). Conversely, some of these amino acids (Gln and Asn) and others like alanine overaccumulated in PPSBdeficient lines. As in shoots, glucose and fructose levels decreased in the roots of SHMT1-deficient lines, with a clear opposite trend to that in the PPSB-deficient lines. These differences in the amino acids and sugar profiles between shoots and roots of PPSB- and SHMT1-deficient lines point to changes in N and C homeostasis between organs in different mutant backgrounds.

To more precisely identify how Ser-Gly homeostasis in shoots and roots was affected by the lack of SHMT1 activity in the PPSB-deficient background, we shifted plants grown under eCO<sub>2</sub> to aCO<sub>2</sub> conditions, where photorespiration is much more active (Fig. 3B; Supplemental Fig. S3). In WT shoots, as expected, the Ser and Gly levels dropped when plants were grown under eCO<sub>2</sub> conditions compared with aCO<sub>2</sub> (Fig. 3B; Supplemental Fig. S3). The Gly/Ser ratio indicated that the drop of Gly levels in shoots under eCO<sub>2</sub> was much greater than that of Ser in both PPSB-deficient and WT lines (Fig. 3B). Other relevant changes found in the shoots of SHMT1-deficient lines shifted from eCO2 to aCO<sub>2</sub> conditions were strong increases in Glu and Asp levels and decreases in 2-oxoglutarate (2-OG) levels (Supplemental Fig. S3). In roots, Gly and Ser levels also decreased in all lines transferred from eCO<sub>2</sub> to aCO<sub>2</sub> conditions, and these changes were more drastic in SHMT1-deficient lines (Fig. 3E; Supplemental Fig. S3). The shift from eCO<sub>2</sub> to aCO<sub>2</sub> primarily affected amino acid homeostasis in roots (Supplemental Fig. S3). In addition to the above-mentioned Gly, the transport amino acids Glu, Gln, Asp, and Asn were more drastically affected in the SHMT1-deficient mutants than in other lines, confirming the influence of photorespiration on amino acid status in roots (Supplemental Fig. S3). Overall, these results indicate that SHMT1 activity has clear consequences for amino acid metabolism and distribution between roots and shoots.

# Root phenotypes in PPSB-deficient lines are dependent on SHMT1/GDC activity in shoots

SHMT1 is mainly expressed in shoots. We performed grafting experiments to elucidate the role of shoots in the changes in root developmental patterns in the mutants. Using the shmt1 c-psp1 shoot as the scion, the root growth of the c-psp1 stock was rescued (Fig. 4; Supplemental Fig. S4), confirming that the changes in developmental patterns in the shmt1 PPSB-deficient lines are shoot-dependent.

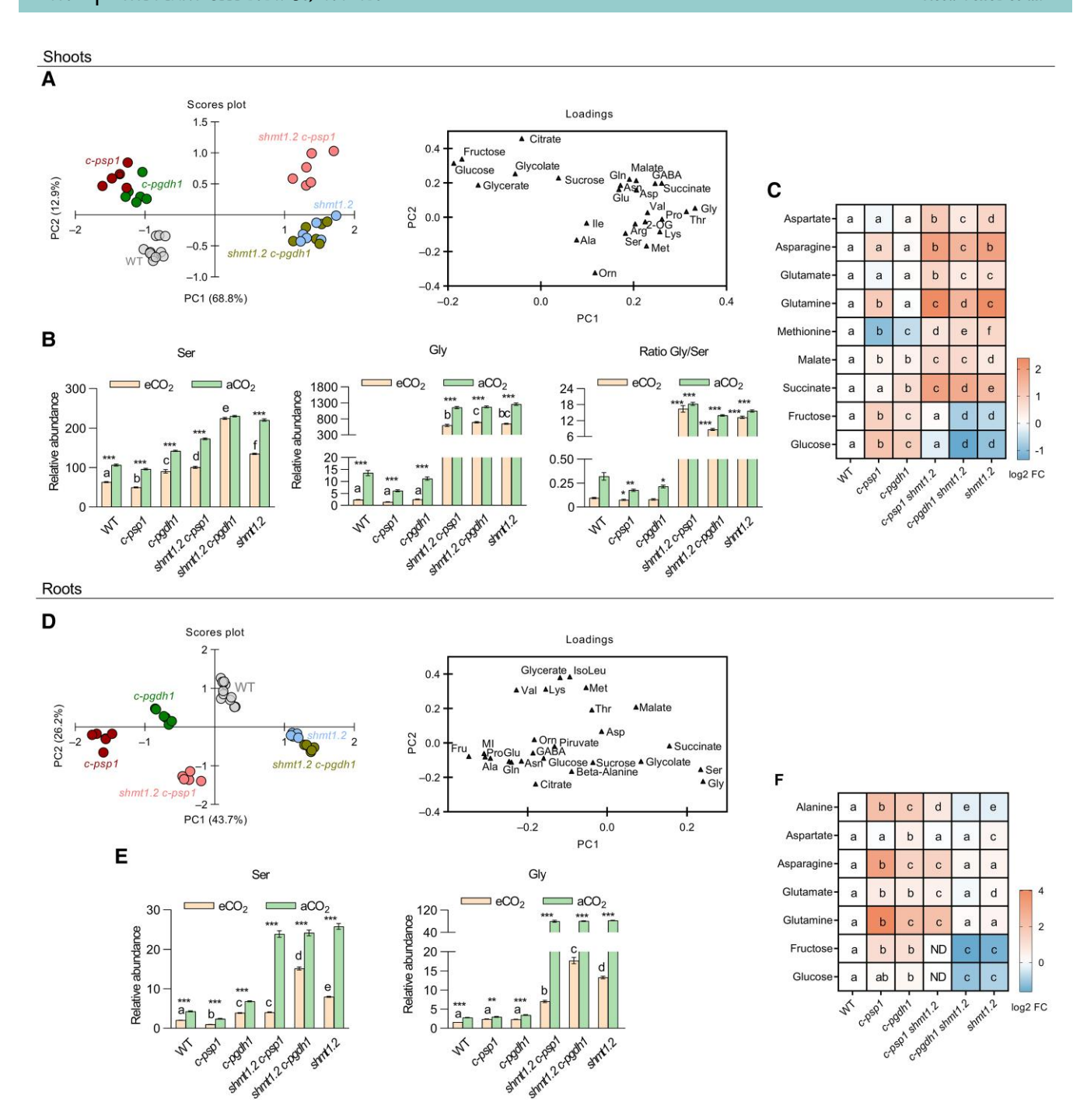


**Figure 3.** Metabolite profiles of WT, PPSB-deficient (c-psp1 and c-pgdh1), and SHMT1-deficient (shmt1.2, shmt1.2 c-psp1, and shmt1.2 c-pgdh1) lines grown under eCO $_2$  conditions. **A** and **D**) PCA and loading plots of metabolites in shoots **A**) and roots **D**). Data from GC-MS analysis were evaluated using PCA with the 2 first components accounting for at least 70% of total metabolic variance. Values in parenthesis give the relative contribution of each component to the total variance observed in the dataset. **B** and **E**) Relative Gly and Ser content in shoots **B**) and roots **E**) of different mutant backgrounds under eCO $_2$  conditions or after a 24 h shift to aCO $_2$  conditions compared with WT. **C** and **F**) Heat map showing most relevant changes in the metabolite contents of shoots **C**) and roots **F**) under eCO $_2$  conditions. Values represent the mean  $\pm$  se,  $n \ge 6$  of pools of 40 plants from 2 different lines for each genotype; different letters indicate significant differences between lines (P < 0.05) under eCO $_2$  conditions; significant differences between the same line under aCO $_2$  and eCO $_2$  conditions, as determined by Student's t-test, are denoted by \* (P < 0.05), \*\* (P < 0.01), and \*\*\* (P < 0.001). In the Gly/Ser ratio, lines are compared with the WT under the same growth conditions.

To investigate the specific role of SHMT1 activity in the observed developmental patterns, we introduced the SHMT2 mutation (shmt2.2, henceforth shmt2) into the PPSB-

deficient lines. SHMT2 is the second mitochondrial SHMT isoform in Arabidopsis. Its activity represents only a very small fraction of total SHMT activity in shoots, which is

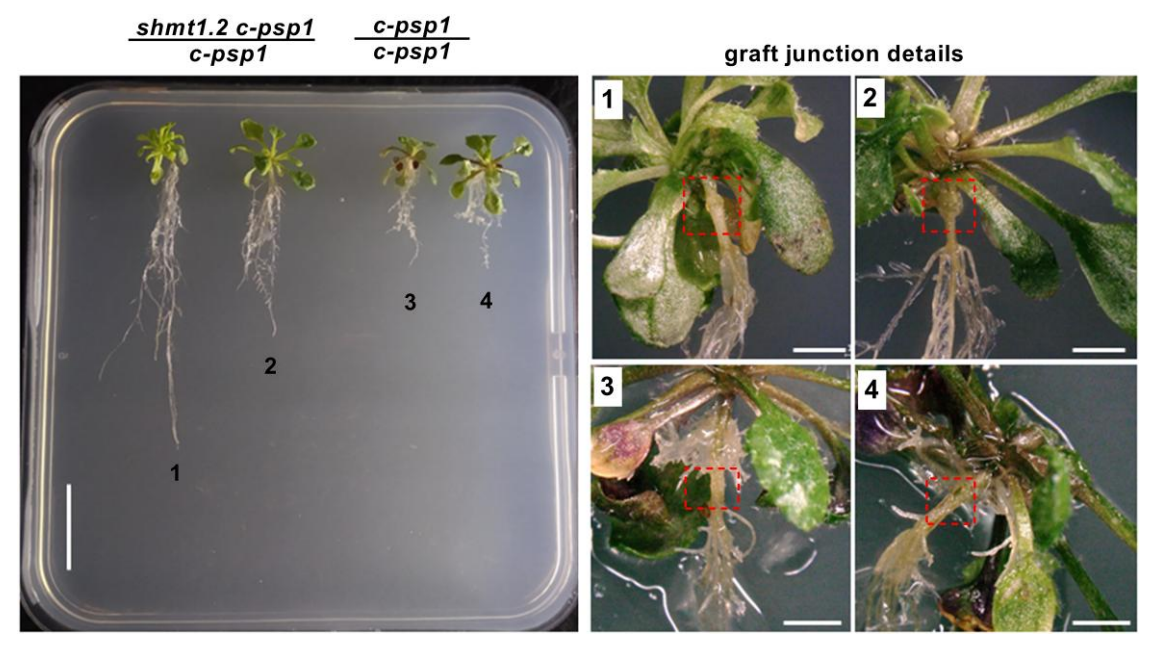


Figure 4. Grafting of scion  $shmt1.2\ c-psp1$  shoots onto c-psp1 roots under eCO<sub>2</sub>. Squares mark the junction between shoots and roots. Scale bars = 2 cm (left) and 2 mm (right).

confined to vascular tissues (Engel et al. 2011) (http://www.bar.utoronto.ca/efp/cgi-bin/efpWeb.cgi). shmt2 c-pgdh1 lines were viable under aCO<sub>2</sub> and eCO<sub>2</sub> conditions, but the SHMT2 mutation did not rescue the inhibited primary root length of c-pgdh1 and even enhanced it under aCO<sub>2</sub> (Supplemental Fig. S5). The most important difference between the shmt1 c-pgdh1 and shmt2 c-pgdh1 mutants was the increase in Ser and especially Gly contents in the shoots of shmt1 c-pgdh1 (Fig. 3B; Supplemental Fig. S5). Overall, these data demonstrate that the change in the developmental patterns observed in shmt1 PPSB-deficient lines is related to the lack of photorespiration-associated SHMT1 activity in shoots.

# 15N labeling experiments confirm that Gly is prioritized over Ser in the double mutants, affecting the Ser-Gly-1c

The <sup>15</sup>N-labeling experiments (Fig. 5) showed that the de novo incorporation of <sup>15</sup>N into Gly was much greater in SHMT1-deficient lines than in WT and *c-pgdh1* (Fig. 5, A and B). However, the de novo incorporation of <sup>15</sup>N into Ser was higher in *c-pgdh1* than in SHMT1-deficient lines, especially in roots. The enrichment of both Gly and Ser, a useful measure of the turnover rate, was lower in the SHMT1-deficient lines than in WT or *c-pgdh1*. However, the enrichment of Ser in SHMT1-deficient lines was much lower than that of Gly (Fig. 5, A and B). Thus, much more Gly is incorporated and is metabolized more quickly than Ser in SHMT1-deficient lines. These data, plus the higher Ser steady-state values, suggest lesser Ser flux into other metabolites in the SHMT1-deficient mutants.

Considering that the differences between the lines with and without SHMT1-deficiency were mostly in the Gly incorporation rate rather than in enrichment, our results suggest that a considerable amount of Gly not being metabolized by SHMT1 is diverted to other metabolic reactions in the mutants. These reactions could include other SHMT isoforms, such as the plastidial SHMT3, whose gene was upregulated in shmt1 c-pgdh1 shoots, or enhanced GDC activity, as deduced by the induction of some genes encoding isoforms of the GDC complex (GLDP1 and GLDP2) in shmt1 c-pgdh1 (Fig. 6). In contrast to shmt1 c-pgdh1, both GDC (GLDP1 and GLDP2) and SHMT1 gene expression was repressed in c-pgdh1 (Figs. 2D and 6C). These results suggest that Gly could also be taken out of the photorespiratory cycle in mitochondria of this mutant at a higher rate than in WT and might be converted to Ser in other compartments or organs to compensate for the Ser deficiency. This notion was substantiated by the greater Gly enrichment found in c-pgdh1 shoots, which indicates a higher Gly metabolization rate (Fig. 5A).

The <sup>15</sup>N flux measurements also indicated that Glu did not display a higher de novo biosynthesis rate in SHMT1-deficient versus PPSB-deficient shoots (Fig. 5A), suggesting that Glu accumulation observed at steady state might be due to lower turnover caused by inhibited photorespiratory flux. However, the de novo <sup>15</sup>N label incorporation into Asp and Asp-derived amino acids such as Met was greater in SHMT1-deficient than in PPSB-deficient shoots. Unlike shoots, <sup>15</sup>N flux analysis in roots indicated greater Asp and Glu biosynthesis in *c-pgdh1* than in *shmt1 c-pgdh1* (Fig. 5B), which could explain the amino acid accumulation in the roots of PPSB-deficient lines.

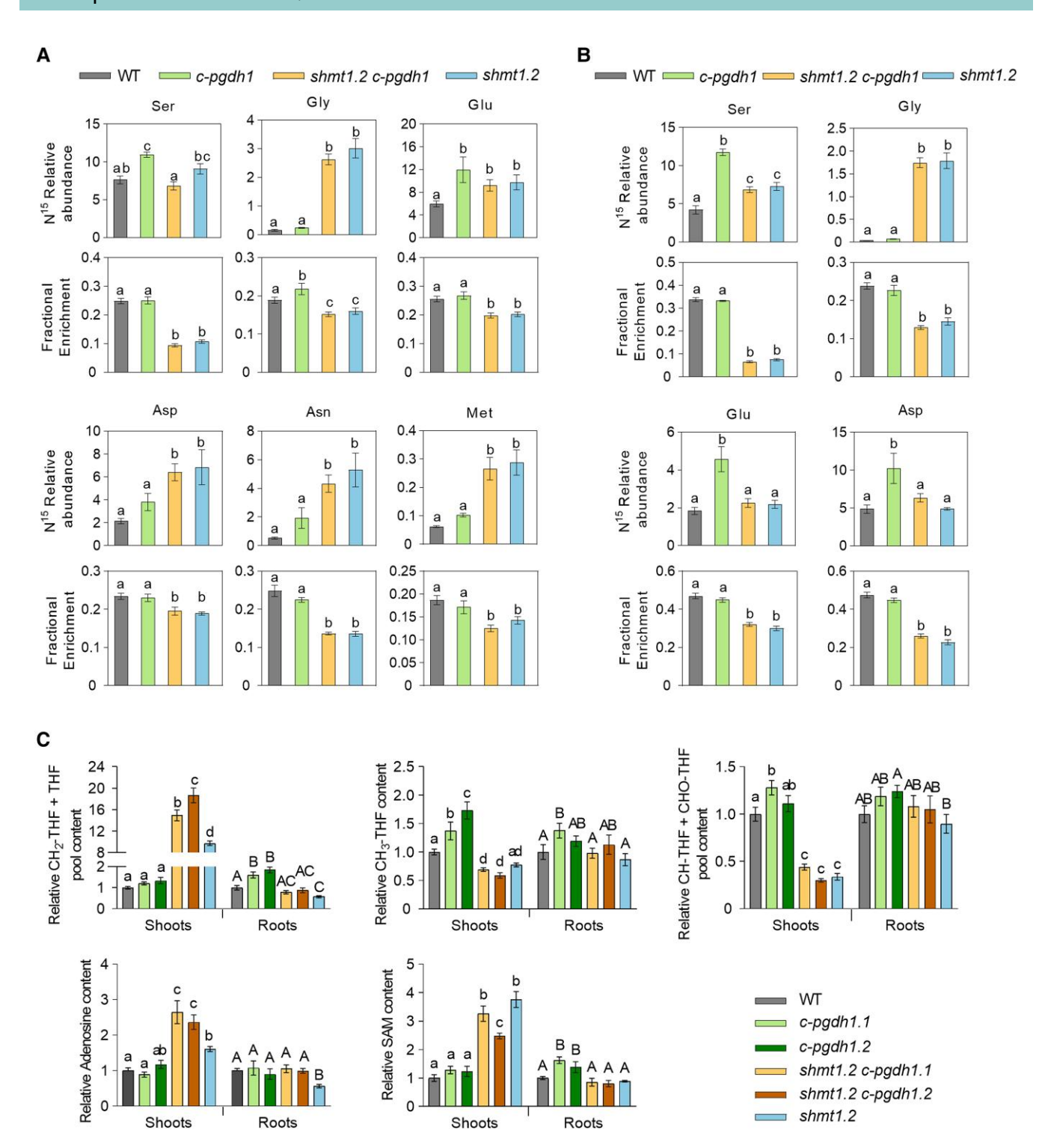
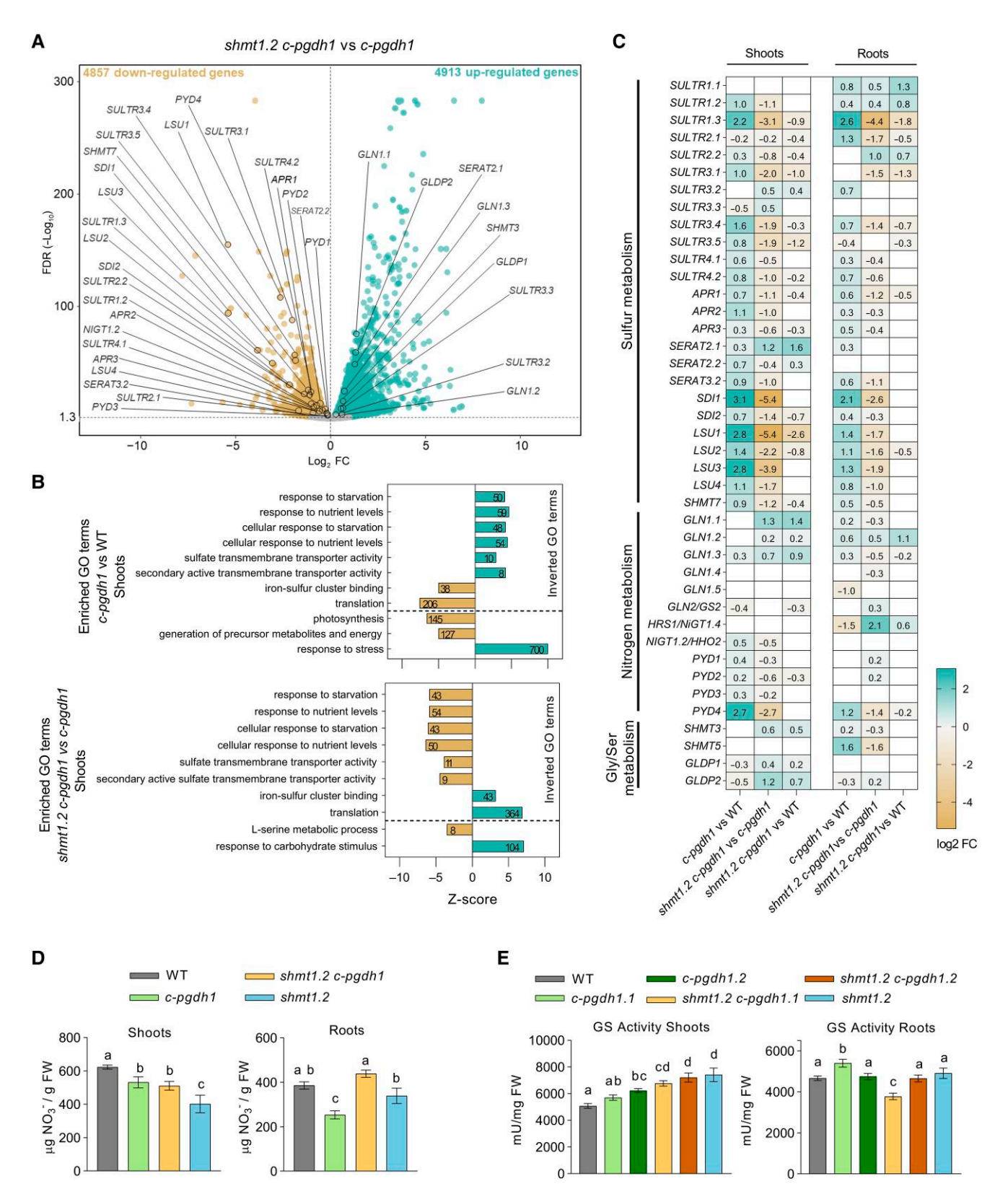


Figure 5. SHMT1-deficient lines (shmt1.2 and shmt1.2 c-pgdh1) incorporate more Gly and Asp-family amino acids and synthesize more folates and SAM intermediates than PPSB-deficient (c-pgdh1) lines. **A** and **B**), Quantification of <sup>15</sup>N-labeled major amino acids in PPSB- and SHMT1-deficient lines grown under eCO<sub>2</sub> conditions; values of shoots **A**) and roots **B**) are shown as relative abundance (upper panel) and fractional enrichment (lower panel). **C**) Relative contents of folate and SAM cycle intermediates in the shoots and roots of different mutant backgrounds grown under eCO<sub>2</sub> conditions compared with WT. In **A**) and **B**), values represent the mean  $\pm$  se,  $4 \le n \le 10$  pools; data represent the mean of at least 45 plants from 2 different lines for each genotype. In **C**), values represent the mean  $\pm$  se,  $n \ge 6$  pools data represent the mean of at least 40 plants. Different letters indicate significant differences between lines (P < 0.05).



**Figure 6.** Transcriptomics profiles of PPSB-deficient (c-pgdh1) and SHMT1-deficient ( $shmt1.2\ c$ -pgdh1) lines under eCO $_2$ . **A)** Volcano plots for differentially expressed genes between  $shmt1.2\ c$ -pgdh1 and c-pgdh1 in shoots. Brown and green dots represent upregulated and downregulated genes, respectively (FDR < 0.05). **B)** Functional category analysis for transcriptional responses in shoots. In each bar, the number of genes differently upregulated or downregulated is shown. **C)** Heat map showing the most relevant changes in the expression of genes related to Gly/Ser, sulfur, and nitrogen metabolism in shoots and roots. Numbers inside boxes stand for log-fold change. **D)** Nitrate ( $NO_3^-$ ) content in shoots and roots of different lines. **E)** Glutamine synthetase (GS) activity in shoots and roots of different lines. Values represent the mean  $\pm$  se,  $4 \le n \le 8$  pools of 40 plants from 2 different lines for each genotype; different letters indicate significant differences between lines (P < 0.05).

Briefly, the most important difference between lines is the higher Gly flux in shoots and roots of SHMT1-deficient lines. The increased Gly flux in shoots of SHMT1-deficient lines is channeled into Asp family amino acids, especially Asn and Met, linking N with S and folate metabolism.

#### Folate and SAM cycles are affected by changes in Ser/ Gly flux

Because Ser and Gly participate in 1C-folate metabolism via SHMT and GDC enzymes, we measured steady-state folate pools. The most striking difference between the lines was the 15-fold higher CH<sub>2</sub>-THF + THF pool size in shmt1 *c-pgdh1* shoots compared with the WT (Fig. 5C). These values are consistent with higher GDC activity in shmt1 c-pgdh1 lines. No method is currently available to distinguish between CH2-THF and THF in plant tissues. However, the increase in the CH2-THF + THF pool in shmt1 and shmt1 c-pgdh1 probably reflects a rise in the level of CH<sub>2</sub>-THF, the product of GDC activity, because shmt1 mutants are unable to convert the CH<sub>2</sub>-THF produced by GDC into Ser and THF in the mitochondria. Other minor changes were found in the folate pool of shmt1 c-pgdh1 shoots, i.e. a reduction in the pools of 5-methyl-THF (CH3-THF) and 5,10-methenyl-THF (CH-THF) + 10-formyl-THF (HCO-THF), with these metabolite levels showing an opposite trend to that in c-pgdh1 shoots. Differences in folate pools between lines were much smaller in roots than in shoots. The CH2-THF + THF pool decreased in *shmt1* roots but increased in *c-pgdh1* roots (Fig. 5C). However, no major changes appeared in the folate levels of shmt1 c-pgdh1 lines, probably due to the balancing of the opposite effects from the 2 single mutants.

The changes in the folate pool found between lines and organs could affect other pathways like the SAM cycle because the methyl moiety of SAM is derived from 1C-folates. The levels of SAM and adenosine, another product of the SAM cycle, increased 2-fold to 3-fold in shoots of SHMT1-deficient lines (Fig. 5C). Increased SAM cycle activity could also explain the depletion of CH<sub>3</sub>-THF, which is the donor of 1C groups for SAM, in SHMT1-deficient lines. Briefly, changes in Ser/Gly flux strongly affected folate and SAM metabolism, modifying the metabolite equilibrium between roots and shoots and affecting S-metabolism.

# Transcriptomic analysis confirms alterations of the N-C-S networks between shoots and roots of *c-pgdh1* and *shmt1 c-pgdh1* lines

In agreement with previous results, PCA of the transcriptomic data indicated that the main differences between lines appeared in shoots and not in roots (Supplemental Fig. S6). When comparing *c-pgdh1* with *shmt1 c-pgdh1* shoots, 4,857 genes were downregulated and 4,913 were upregulated (Fig. 6A). Compared with WT, in *c-pgdh1* shoots, several categories of genes related to response to nutrient level and starvation were upregulated, including marker genes for S and N deficiency (Fig. 6B). When comparing *shmt1 c-pgdh1* 

with *c-pgdh1*, however, genes in the same categories that respond to nutrient levels were downregulated. In shoots of *c-pgdh1*, there was a general induction of genes encoding enzymes participating in pyrimidine catabolism, the so-called *PYD* genes, which respond to N deficiency (Fig. 6C; Supplemental Fig. S7). In particular, *PYD4*, the last gene of the pyrimidine catabolic pathway, was strongly upregulated in *c-pgdh1* lines and strongly repressed in *shmt1 c-pgdh1*. *PYD* genes are induced under N-limited conditions to use pyrimidines as an N source (Zrenner et al. 2009; Witte and Herde 2020). Accordingly, downregulation of genes encoding enzymes participating in the biosynthesis of pyrimidine intermediates occurred in *c-pgdh1* shoots compared with WT, while the opposite trend was noted when comparing *shmt1 c-pgdh1* lines versus *c-pgdh1* (Supplemental Fig. S7).

In roots, the HSR1/NIGT1.4 was strongly downregulated in c-pgdh1 but upregulated in shmt1 c-pgdh1 compared with the WT (Fig. 6C). HSR1/NIGT1.4 is a member of the NIGT clade that is specifically expressed in roots, encoding a transcriptional repressor of the NO<sub>3</sub><sup>-</sup> transporter gene NTR2.1 (Maeda et al. 2018; Ueda et al. 2020). The downregulation of HSR1/NIGT1.4 in c-pgdh1 roots suggests that NO<sub>3</sub><sup>-</sup> uptake was activated as a response to N deficiency. Accordingly, the NO<sub>3</sub> content in *c-pgdh1* roots was approximately 35% lower than in WT (Fig. 6D), while the NO<sub>3</sub> content in shmt1 c-pgdh1 roots was significantly higher than that of c-pgdh1 and similar to that of WT (even a 14% increase was observed). Another NIGT clade member, NIGT1.2, was upregulated in c-pgdh1 shoots and downregulated in shmt1 c-pgdh1 shoots compared with c-pgdh1. These data show that NO<sub>3</sub> signaling between shoots and roots is differentially altered in PPSB-deficient and SHMT1-deficient lines, probably reflecting a change of NO<sub>3</sub><sup>-</sup> allocation between the organs. The gene expression pattern of glutamine synthetase (GS) isoforms was also altered in c-pgdh1 versus shmt1 c-pgdh1. Major changes occurred in the cytosolic GS isoforms GLN1.1, GLN1.2, and GLN1.3, showing an opposite expression pattern between shoots and roots (Fig. 6C).

NH<sub>4</sub><sup>+</sup> content showed a similar increase in shoots of both *c-pgdh1* and *shmt1 c-pgdh1* mutant lines compared with WT (Supplemental Fig. S8). To determine whether this higher NH<sub>4</sub><sup>+</sup> content was related to changes in a biosynthetic process, we measured GS activity. Compared with the WT, GS activity was greater in *shmt1 c-pgdh1* shoots, but similar to or even lower than that in *c-pgdh1* roots (Fig. 6E). These results indicate that N signaling between shoots and roots is altered in *shmt1 c-pgdh1* compared with *c-pgdh1*, confirming that SHMT1 activity can profoundly affect N homeostasis.

Genes encoding sulfate transporters (SULTRs) and proteins involved in S metabolism in general were downregulated in *shmt1 c-pgdh1* shoots compared with *c-pgdh1* (Fig. 6B). Thus, genes described as S deficiency markers, such as SHMT7, LSU1, LSU2, LSU3, LSU4, SDI1, and SDI2, which were upregulated in *c-pgdh1* shoots and roots compared with WT, showed the opposite trend in *shmt1 c-pgdh1*. Some of these genes (LSU1, LSU2, SHMT7, and SDI2) showed

**Table 1.** Carbon (C), nitrogen (N), and sulfur (S) contents (mg/g dry weight) in shoots and roots of WT, PPSB-deficient (*c-pgdh1*), and SHMT1-deficient (*shmt1.2 c-pgdh1*, *shmt1.2*) lines growth under eCO<sub>2</sub> conditions

genotype	C	N	S	N/C ratio	S/C ratio
			Shoots		
WT	$400.1 \pm 0.6^{a}$	$67.86 \pm 0.27^{a}$	$9.12 \pm 0.15^{a}$	$0.170 \pm 5.49 \cdot 10^{-4}$ a	$0.023 \pm 4.03 \cdot 10^{-4}$ a
c-pgdh1	$419.9 \pm 0.7^{b}$	$62.80 \pm 0.41^{b}$	$7.37 \pm 0.12^{b}$	$0.150 \pm 9.04 \cdot 10^{-4}$ b	$0.018 \pm 3.08 \cdot 10^{-4}$ b
shmt1.2 c-pgdh1	$390.5 \pm 1.0^{\circ}$	$70.69 \pm 0.29^{c}$	$10.84 \pm 0.10^{\circ}$	$0.181 \pm 7.75 \cdot 10^{-4}$ c	$0.028 \pm 3.26 \cdot 10^{-4}$ c
shmt1.2	$397.2 \pm 3.0^{a}$	$69.90 \pm 0.26^{\circ}$	11.57 ± 0.26 <sup>d</sup>	$0.176 \pm 3.42 \cdot 10^{-3}$ c	$0.029 \pm 8.17 \cdot 10^{-4}$ c
			Roots		
WT	$418.8 \pm 0.7^{a}$	$51.75 \pm 0.34^{a}$	$7.30 \pm 0.09^{a}$	$0.124 \pm 7.68 \cdot 10^{-4}$ a	$0.017 \pm 2.25 \cdot 10^{-4}$ a
c-pgdh1	$427.9 \pm 0.8^{b}$	54.92 ± 0.16 <sup>b</sup>	$9.77 \pm 0.07^{b}$	$0.128 \pm 5.18 \cdot 10^{-4}$ b	$0.023 \pm 1.36 \cdot 10^{-4}$ b
shmt1.2 c-pgdh1	$403.8 \pm 0.1^{\circ}$	$57.45 \pm 0.40^{\circ}$	$8.97 \pm 0.10^{\circ}$	$0.142 \pm 1.08 \cdot 10^{-3}$ c	$0.022 \pm 2.35 \cdot 10^{-4}$ b
shmt1.2	413.7 ± 1.2 <sup>d</sup>	57.12 ± 1.31 <sup>c</sup>	$7.39 \pm 0.22^{a}$	$0.138 \pm 2.78 \cdot 10^{-3}$ d	$0.018 \pm 4.85 \cdot 10^{-4}$ c

Values represent the mean  $\pm$  ss,  $n \ge 6$  of pools of 40 plants from 2 different lines per genotype; different letters ( $^{a, b, c, d}$ ) indicate significant differences between lines (P < 0.05).

even lower expression levels in shmt1 c-pgdh1 shoots than in the WT, which agrees with the notion that S metabolism is activated in these mutant lines (Fig. 6C). SULTRs and adenosine phosphosulfate reductase (APR) enzymes play predominant roles in controlling sulfate assimilation in plastids (Ristova and Kopriva 2022). All 3 APR genes were upregulated in c-pgdh1 compared with WT but downregulated in shmt1 c-pgdh1 compared with c-pgdh1 (Fig. 6C). SULTR genes showed different expression patterns depending on their functions in plants. SULTR1.1 and SULTR1.2, whose major functions involve root uptake, were upregulated in roots of both c-pgdh1 and shmt1 c-pgdh1, but with higher expression levels in the latter (Fig. 6C). However, an opposite expression trend appeared in most of the other 10 SULTR genes in both mutants, especially in shoots. Notably, SULTR1.3 and SULTR3.1 were highly upregulated in c-pgdh1 and highly downregulated in shmt1 c-pgdh1. SULTR1.3 is a high-affinity SULTR required for sulfate uptake and for maintaining S metabolism in the sieve element companion cell complex (Yoshimoto et al. 2007). Deletion of this high-affinity SULTR restricted transfer of <sup>35</sup>S from cotyledons to shoot meristems and roots in Arabidopsis (Yoshimoto et al. 2007). SULTR3.1 participates in sulfate transport at chloroplast/plastid envelopes (Cao et al. 2013). Taken together, these transcriptional data indicate that the expression of genes responding to sulfate signaling and sensing was altered in shmt1 c-pgdh1 compared with c-pgdh1, with the upregulation of major sulfate uptake transporter genes in roots but downregulation of APR genes, and most SULTR genes involved in intercellular and intracellular sulfate transport.

Unlike genes that respond to nutrient levels, genes related to carbohydrate metabolism were among the most highly upregulated in *shmt1 c-pgdh1* shoots (Fig. 6B). For example, among the 154 differentially regulated genes in the "response to carbohydrate stimulus" category in *shmt1 c-pgdh1* shoots, 104 were upregulated (Fig. 6B; Supplemental Data Set 1). This also indicates a shift in C metabolism between *c-pgdh1* and *shmt1 c-pgdh1*. Therefore, we measured total N, C, and S levels in roots and shoots (Table 1). In *c-pgdh1*, an alteration occurred in the distribution of S and N between shoots and roots versus WT, with a deficiency in shoots and an

excess in roots. However, the C content increased in both shoots and roots of c-pgdh1 versus WT. In shmt1 c-pgdh1, however, the S and N contents increased in shoots to levels even higher than in the WT, but the C content decreased in both shoots and roots. The most important differences between shmt1 c-pgdh1 and c-pgdh1 were, once again, found in shoots, particularly in the S content. Compared with the WT, the S content of *c-pgdh1* shoots decreased by approximately 20% but increased by ~20% in shmt1 c-pgdh1, following a similar trend in shmt1. Due to the changes in C, S, and N contents, the N/C and S/C ratios in shoots decreased in PPSB-deficient lines and increased in SHMT-deficient lines. In roots, the most important differences between both lines were changes in the C content, which dropped in shmt1 c-pgdh1 and rose in c-pgdh1. We also measured total N, S, and C contents under aCO<sub>2</sub> growth conditions in the c-pgdh1 line, confirming that the reduction in N and S contents and the increase in C content in shoots of the PPSB-deficient lines occurred independently of photorespiratory activity (Supplemental Table S1).

Therefore, the deficiency of N and S that occurred in *c-pgdh1* shoots was corrected by bypassing the photorespiratory flux at the SHMT1 level. This implies that PGDH1 and SHMT1 activities play important roles in regulating C, N, and S distribution within and between plant cells and organs.

# Protein and carbohydrate metabolism is differentially affected in PPSB- and SHMT-deficient lines

We performed protein biosynthesis experiments using a labeled <sup>35</sup>SCys/<sup>35</sup>SMet cocktail in shoots. Neither *c-pgdh1* nor *shmt1 c-pgdh1* showed higher amino acid incorporation into proteins than WT (Fig. 7A). However, the enrichment of <sup>35</sup>SCys/<sup>35</sup>SMet was lower in SHMT1-deficient lines than in WT or *c-pgdh1*, which suggests a lower metabolization rate. This could indicate a greater preference of N-containing metabolites as a C sink instead of carbohydrates and would agree with the increased N and S and the decreased soluble sugar contents in these lines. We checked the growth responses of *c-pgdh1* and *shmt1 c-pgdh1* in the presence of exogenous 2% sucrose. While the shoot fresh weight of *shmt1* 

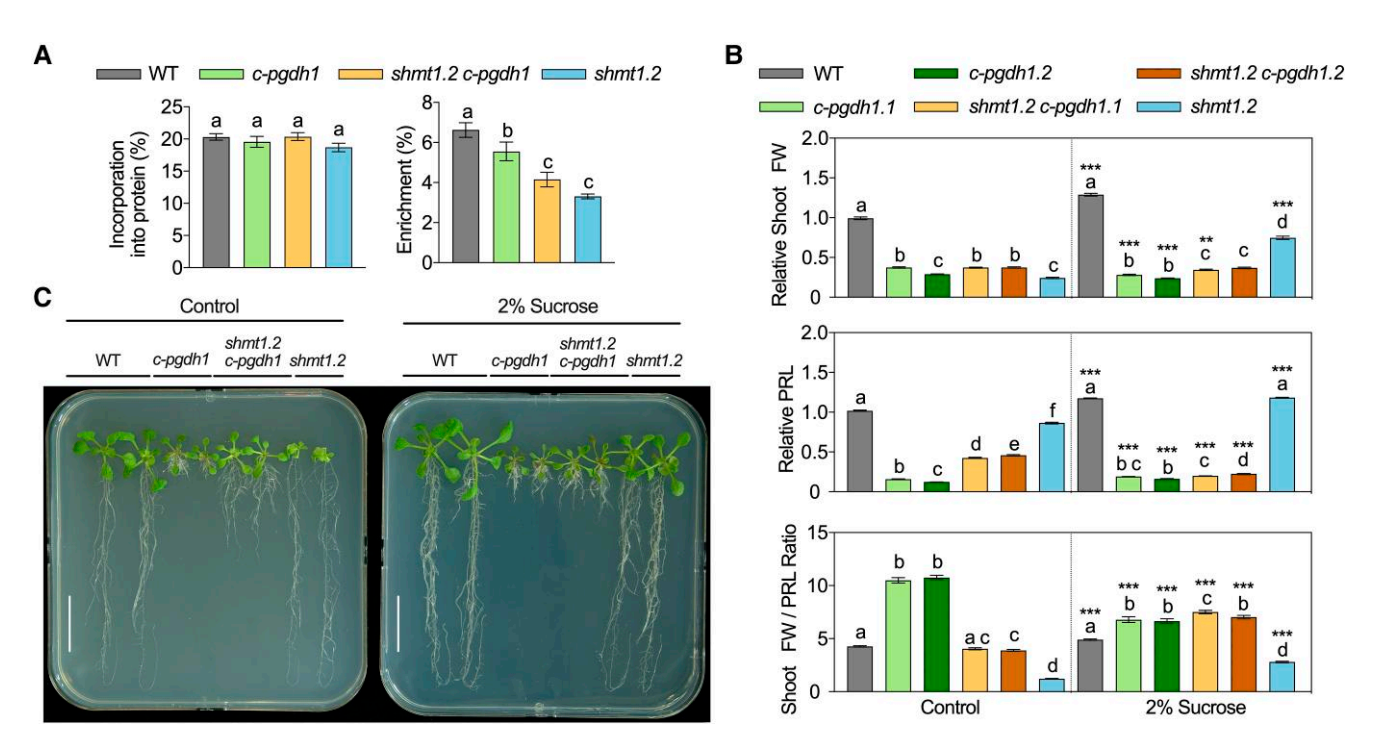


**Figure 7.** Protein and carbohydrate metabolism is differentially affected in PPSB-deficient (c-pgdh1) and SHMT1-deficient (shmt1.2 and shmt1.2 c-pgdh1) lines under eCO $_2$  conditions. **A)** Protein synthesis in shoots measured by  $^{35}$ S-Met/ $^{35}$ S-Cys labeling experiments. Values are shown as incorporation into proteins (left panel) and enrichment (right panel). **B)** Relative shoot fresh weight (FW), primary root length (PRL), and shoot FW/PRL ratio of different lines supplemented  $\pm 2\%$  sucrose. **C)** Photograph of representative individuals of each line. In **A)**, values represent the mean  $\pm sE$ ,  $n \ge 6$  pools of 40 plants from 2 different lines for each genotype; different letters indicate significant differences between lines (P < 0.05). In **B)**, values (mean  $\pm sE$ ;  $n \ge 40$  plants from 2 different lines for each genotype) are normalized to the mean calculated for the WT. Different letters indicate significant differences between lines (P < 0.05); significant differences between the same line under control growth conditions, as determined by Student's t-test, are denoted by \* (P < 0.05), \*\* (P < 0.01), or \*\*\* (P < 0.001). Scale bars = 2 cm (C).

increased almost 3-fold, the shoot growth of c-pgdh1 was negatively affected by this treatment (Fig. 7, B and C). Interestingly, sucrose treatment drastically decreased the primary root length of shmt1 c-pgdh1 but increased the primary root length of c-pgdh1 (Fig. 7, B and C). Consequently, sucrose treatment altered the plant developmental pattern depending on the genetic background, as shown by the shoot fresh weight/primary root length ratio, which increased in the SHMT-deficient lines but decreased in c-pgdh1 compared with control medium without sucrose (Fig. 7B). These results confirm the notion that SHMT1-deficient lines have impaired carbohydrate metabolism compared with the other lines and that developmental changes in PPSB- and SHMT-deficient mutants involve nutrient sensing and signaling mechanisms in different plant organs, as well as shootroot communications processes.

#### **Discussion**

Evidence supports the involvement of photorespiratory Gly in the maintenance of Ser homeostasis at the whole plant level

Crosstalk has been proposed between photorespiration and PPSB during Ser biosynthesis. This assumption is based on

the observation that Ser levels drop to a lesser extent than Gly levels under low photorespiratory conditions in WT leaves (Kleczkowski and Givan 1988; Fig. 3B), which might be due to PPSB induction when photorespiration is compromised (Modde et al. 2017; Fig. 2, C and D). However, we have shown that steady-state levels of Ser also drop to a much lesser extent than Gly in PPSB-deficient lines under photorespiratory-reduced conditions (Fig. 3B). We have also shown that not only Gly but also steady-state Ser levels increase in double mutants devoid of PGDH and SHMT1 activities. 15N-flux measurements indicated that less Ser was incorporated into shoots and roots in the shmt1 c-pgdh1 lines than in PPSB-deficient lines (Fig. 5, A and B), as expected after eliminating the major enzymes responsible for its synthesis. Therefore, we propose that some of the Gly leaving photorespiration is used for Ser synthesis in the cytosol and plastids. This conversion of Gly into Ser through cytosolic and plastidial SHMTs is not thermodynamically favored. However, the high Gly/Ser ratio in the SHMT1-deficient lines could shift the reaction equilibrium in favor of Ser formation in these compartments.

Gly and Ser levels in roots also decreased in all lines in response to the transition from aCO<sub>2</sub> to eCO<sub>2</sub> conditions, especially in SHMT1-deficient lines. This implies that fractions of the root Gly and Ser pools are also associated with

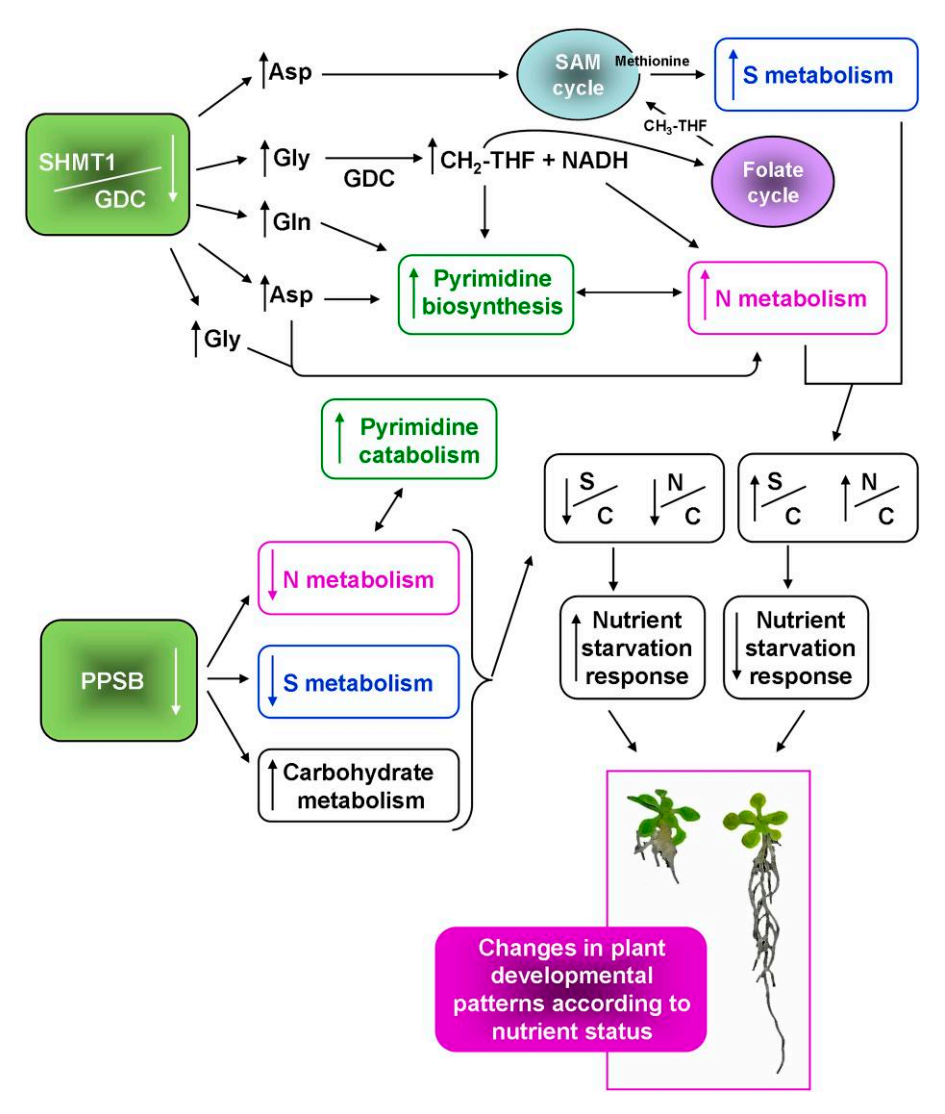


**Figure 8.** Proposed model for metabolic pathways interacting with the PPSB and GPSB. Reduced PPSB activity negatively affects nitrogen (N) and sulfur (S) metabolism in shoots and induces the nutrient starvation response. Lack of SHMT1 activity increases glycine, aspartate as well as CH<sub>2</sub>-THF content, which has an impact on pyrimidine metabolism, activating biosynthetic and repressing catabolic processes. SAM is also activated. All these changes, along with possible increases in NADH content, positively affect N, S, and carbon (C) metabolism, repress the nutrient starvation response, and change the N/C and S/C ratios, which modify the plant developmental pattern. Enzymes: GDC, glycine-decarboxylase complex; SHMT1, serine-hydroxymethyl transferase 1. Metabolites: CH<sub>3</sub>-THF, 5-methyl-THF, Asp, aspartate; CH<sub>2</sub>-THF, 5,10-methylene-THF; GIn, glutamine.

photorespiratory activity, suggesting that both amino acids are transported from shoots to roots. These data collectively indicate the involvement of photorespiratory Gly in maintaining Ser homeostasis at the whole plant level. Thus, the regulation of SHMT/GDC activity could be a crucial component of the contribution of photorespiration to Ser–Gly–1C homeostasis in plants. The provision of more or less Gly from photorespiration could be a physiological strategy, as suggested by the downregulation of SHMT1 and GDC genes in PPSB-deficient lines to provide Ser and folates for growth and metabolism when other pathways such as the PPSB are restricted. However, other questions remain. For instance, why do PPSB-deficient mutants have such strong phenotypes? Thus, the vast majority of the observed metabolic

changes in PPSB-deficient lines may not be related to Ser starvation directly, which was not always observed in PPSB-deficient lines, but are most likely caused by alterations in nutrient signaling and metabolism. As we have shown that changes in shoots are responsible for the phenotypes of roots (Fig. 4), our results suggest that metabolic changes in shoots led by Gly might modulate root development (Fig. 8).

#### Folates and Gly as activators of N metabolism

Photorespiration was long considered to be a process that reduces photosynthetic efficiency, especially in C<sub>3</sub> plants, and considerable efforts have been made to reduce its activity or bypass the metabolic pathway (the so-called photorespiratory bypasses) in order to enhance crop productivity

418

(Kebeish et al. 2007; Peterhansel et al. 2010; Betti et al. 2016; Cotton et al. 2018; Shen et al. 2019; South et al. 2019; Baslam et al. 2020; Fernie and Bauwe 2020). However, several studies have indicated that reduced photorespiratory rates due to the increasing atmospheric CO<sub>2</sub> concentrations will positively affect plant biomass (Ainsworth and Long 2020), most likely causing a decrease in their nutritional quality (Myers et al. 2014; Medek et al. 2017). Our study supports the notion that regulating photorespiratory activity might provide benefits for N, S, and folate status, which is important for the nutritional quality of crops.

One of the main problems associated with increasing atmospheric CO<sub>2</sub> levels is the reduction in N and protein contents in plants, which alters the N/C ratio (Wieser et al. 2008; Bloom et al. 2010; Myers et al. 2014; Medek et al. 2017; Bloom et al. 2020). Under eCO<sub>2</sub> conditions, N content is constrained in leaves of C<sub>3</sub> plants but not in roots (Jauregui et al. 2016). PPSB-deficient lines also showed altered N and S allocation between roots and shoots (lower in shoots and higher in roots than in WT; Table 1). In shmt1 c-pgdh1 shoots, however, the N and S content increased, and marker genes for S and N deficiency were downregulated (Table 1 and Figs. 6, B and C). Thus, our data demonstrate that a shift in photorespiratory flux affects the N status in shoots of PPSB-deficient plants at the transcriptional and metabolic levels, corroborating the important impact of photorespiration on N metabolism.

How the N/C ratio is altered by eCO<sub>2</sub> has been the subject of intense debate in recent years (Bloom et al. 2010, 2012, 2014; Bloom 2015; Jauregui et al. 2015, 2016; Walker et al. 2016; Eisenhut et al. 2019; Andrews et al. 2020). Diminished photorespiratory flux has been suggested as one of the possible causes of reduced NO<sub>3</sub><sup>-</sup> assimilation (and uptake) in shoots, although the mechanism is not fully understood (Rachmilevitch et al. 2004; Bloom 2015; Krämer et al. 2022). One plausible hypothesis to explain the relationship between photorespiration and NO<sub>3</sub><sup>-</sup> assimilation points to the high demand for electrons required to power NO<sub>3</sub><sup>-</sup> reduction by nitrate reductase. Bloom and Lancaster (2018) postulated an alternative photorespiratory pathway that increases photorespiratory energy efficiency by generating malate in the chloroplast. Low photorespiratory activity under eCO<sub>2</sub> could impair the malate: 2-OG shuttle in the chloroplast, decreasing the reducing power in the form of NADH in the cytosol for nitrate reductase activity (Bloom and Lancaster 2018; Shi and Bloom 2021). In shmt1 c-pgdh1 lines, we did not find any differences in the levels of glycolate (Supplemental Fig. S2), one of the products of the postulated alternative photorespiratory reaction, which could explain changes in the N status between lines.

Alternatively, other sources of higher NADH content in shmt1 c-pgdh1 could increase the reducing power for nitrate reductase activity in these lines. In shmt1 c-pgdh1 lines, photorespiration is arrested before the hydroxypyruvate reductase reaction; this enzyme consumes NADH in the peroxisome (Fig. 1). Besides, shmt1 c-pgdh1 lines showed increased GDC gene expression in shoots (Fig. 6C), which

could provide extra NADH in mitochondria. Therefore, excess NADH levels in the mitochondria and peroxisomes of shmt1 c-pgdh1 could also help provide the NADH required for nitrate reductase activity in the cytosol through the malate shuttles. Supporting this idea, shmt1 c-pgdh1 displayed higher malate levels compared with the other lines.

Increases in the levels of other metabolites associated with SHMT1/GDC activity in SHMT1-deficient shoots, such as Gly itself and those of the  $CH_2$ -THF + THF pool (Figs. 3B and 5C), could also have an impact on N and S metabolism. The overaccumulation of Gly in SHMT1-deficient lines may play a key role in stabilizing the C/N balance by consuming photosynthetic products and providing amino groups for N metabolism. It has been suggested that, under photorespiratory conditions, plants divert a considerable amount of C into amino acids such as Gly and Ser, which in turn stimulate amino acid biosynthesis and N assimilation (Busch et al. 2018). As described by Abadie et al. (2016), the Gly/Ser stoichiometry of photorespiration is close to 2 but increases at high photorespiratory rates. Thus, subtle changes in SHMT1/GDC catalytic activity would build up Gly, sequestering N, which would need to be compensated for by increased N assimilation (Abadie et al. 2016). Photorespiratory flux is up to 100-fold greater than NO<sub>3</sub> reduction (Bloom et al. 2010), so even a slight imbalance in photorespiratory recycling may affect the plant N budget. By increasing the availability of Gly, we modified N/C and S/C ratios in plants, confirming earlier predictions.

It has been hypothesized that the deposition of already fixed N as Gly is important for effective de novo N assimilation, because Gly (and Ser) are N sinks with low C content, leaving C skeletons (2-OG) available for de novo N assimilation (Krämer et al. 2022). SHMT1-deficient lines divert a large amount of Gly from the photorespiratory cycle compared with other lines, which affects N accumulation in shoots (Fig. 5A and Table 1). Besides, Gly is metabolized more quickly in PPSB-deficient mutants than in other lines, likely to obtain Ser, which may account for their lower N content in shoots under both photorespiratory and nonphotorespiratory conditions. Since high photorespiratory rates stimulate NO<sub>3</sub> assimilation and uptake in plants (Rachmilevitch et al. 2004; Bloom 2015), high Gly levels (or metabolites derived from Gly) in shoots may positively affect root NO<sub>3</sub> uptake, as suggested by the increased NO<sub>3</sub> content in roots of shmt1 c-pgdh1 (Fig. 6D). If this were so, the drop in Gly content observed when WT plants grow under eCO<sub>2</sub> could be one of the signals to reduce N assimilation. As Gly and Ser contents in plant cell are lower than the contents of other major amino acids, Gly/Ser status may not serve as an N reservoir but may instead function as the metabolic signal to modulate NO<sub>3</sub> uptake and assimilation.

The high Gly contents in the SHMT1-deficient lines led to a change in the folate content, especially the CH<sub>2</sub>-THF + THF pool (Fig. 5C), most likely indicating an increase in the CH2-THF content. Thus, photorespiration might also be related to N metabolism via its impact on folate metabolism.

Folates were reported to play important roles in signaling cascades (Stokes et al. 2013), as well as in N and C metabolism (Jiang et al. 2013; Meng et al. 2014; Li et al. 2021), but the action mechanisms remain largely unknown. Folates are substrates for the synthesis of purines and pyrimidines; these major N-containing molecules are required for DNA and RNA biosynthesis. Transcriptomic data indicate that the pyrimidine catabolism pathway was strongly upregulated in c-pgdh1 lines (Supplemental Fig. S7), likely as a response to organic N depletion, while pyrimidine biosynthesis was downregulated. The large supply of CH<sub>2</sub>-THF, Gln, and Asp in the SHMT1-deficient lines, which are all required for pyrimidine biosynthesis, could fuel the pyrimidine biosynthetic pathway and restore the N balance in cells. These data allow us to hypothesize that Gly, along with the 1C-folate pathway, acts on nutrient signaling networks leading to the regulation of N metabolism and represents links between photorespiration and N metabolism (Fig. 8).

Overall, our results support the idea that the regulation of SHMT1/GDC may play a key role in the crosstalk between photorespiration and N-metabolism. Much speculation has been made as to why low photorespiration rates reduce N and protein contents. Our results provide genetic evidence for the biological relevance of regulating SHMT1/GDC activity on N metabolism (Fig. 8). We also provide clues about the underlying molecular mechanisms.

### SHMT1/GDC activity links S with folate and SAM metabolism

The molecular mechanisms controlling S sensing and signaling in plants are not fully elucidated. We show that changes in the Gly/Ser flux alter the metabolic and transcriptional responses to S (Figs. 5C, 6B, and 6C). At the transcriptional level (Fig. 6, B and C), sulfate signaling and sensing were altered in shmt1 c-pgdh1 in an opposite manner to that in c-pgdh1, pointing to the importance of the PPSB-GPSB interaction for balancing S homeostasis between heterotrophic and autotrophic tissues and also between cellular compartments. 1C units are required to synthesize the S-containing amino acid Met (Fig. 1) and could thus be involved in the activation of S-metabolism in shoots of SHMT1-deficient lines. SHMT1-deficient lines showed high levels of CH2-THF+ THF but reduced levels of other THF forms such as CH<sub>3</sub>-THF or CH-THF (Fig. 5C). This finding suggests that there is not equilibrium between different THF pools among plant cell compartments. Alternatively, changes in folate homeostasis could be related to the activation of other metabolic pathways in SHMT1-deficient lines, such as the SAM cycle in the cytosol (Ravanel et al. 2004). The levels of SAM cycle components adenosine, SAM, and Met increased in SHMT1-deficient lines compared with the WT (Fig. 5C). SAM not only serves as a methyl donor in methylation reactions, but it is also an important S-containing metabolite and a form of reduced S that undergoes long-distance transport (Rennenberg et al. 1979; Bonas et al. 1982; Lappartient et al. 1999; Davidian and Kopriva 2010; Tan et al. 2010; Watanabe et al. 2021). Thus, the S-containing metabolites of the SAM cycle could be the link between SHMT/GDC activity and S metabolism.

Our results suggest that Asp and its derived amino acids may participate in bottleneck reactions in the shoots of shmt1 PPSB-deficient lines. Under eCO<sub>2</sub> conditions, Asp levels increased in all lines, as expected, since photorespiration drains amino groups out of the Asp pools (Novitskaya et al. 2002). However, under these eCO2 conditions at which SHMT1deficient lines are viable, we found higher de novo incorporation of Asp as well as much higher Asp pools in shoots of SHMT1-deficient lines than in other lines (Figs. 3C and 5A). This greater incorporation could be directly related to the increased accumulation of Glu in these lines, from which Asp is formed. Increased levels of SAM cycle metabolites might also be involved in the activation of the Asp pathway (or vice versa) in SHMT1-deficient lines. Indeed, the Asp pathway is finely regulated by SAM and Cys feedback loops (Sauter et al. 2013; Galili et al. 2016). Asp is a precursor of the essential amino acids Met, lysine, threonine, and isoleucine and of nucleotides and NAD+, which serve as key metabolites for cell proliferation. This coregulation is consistent with the changes in folate levels in shoots and roots of SHMT1-deficient lines and supports the connection between folates and the S metabolism. Taken together, we can reasonably infer that the change in Asp concentration is one of the key reasons for the metabolic changes observed in SHMT1-deficient lines. To date, the mechanisms controlling Asp homeostasis are not fully elucidated. Thus, our results may reveal an important link between Asp and the regulation of SHMT1/GDC activity. We propose that this connection links photorespiration to S metabolism through the folate and SAM cycles (Fig. 8).

# Crosstalk of C, S, and N metabolism shapes root development

In contrast to amino acids, glucose and fructose levels were drastically reduced in the mutants with a SHMT1-deficient background (Fig. 3C). The low hexose levels in SHMT1deficient lines could not only be explained by slow recycling of photorespiration-derived 3-PGA (Eisenhut et al. 2017; Flügel et al. 2017; Timm et al. 2021) but also by their greater use in the synthesis of Asp family amino acids, as shown in mammals (Ritterhoff et al. 2020). The lower turnover of proteins in shmt1 c-pgdh1 could mean that these lines prioritize protein accumulation as sink to the detriment of other metabolites such as sugars in order to channel the excess amino acids. In the end, the upregulation of genes responding to carbohydrate stimulus and the reduction in total C content in shmt1 c-pgdh1 are consistent with a C deficiency in SHMT1-deficient lines. In *c-pgdh1*, however, there is an excess of C (glucose, fructose, and total C; Fig. 3C and Table 1), likely due to the lack of 3-PGA utilization for Ser synthesis by PGDHs.

These lines also showed a deficiency of S and N in shoots. We propose that the imbalanced S/C and N/C ratios might

affect root growth in PPBS mutants (Fig. 8). The strong reduction in primary root growth in the shmt1 c-pgdh1 mutant in the presence of sucrose corroborated this hypothesis. Since one of the inhibitory effects of sucrose on photosynthesis is the inhibition of Rubisco activity itself (Quentin et al. 2013; Lobo et al. 2015), we assume that, under these growth conditions, photorespiration may be further inhibited, while plants maintain high levels of C provided by sucrose. Changes in the developmental pattern in the shmt1 c-pgdh1 mutant could therefore be explained by the following: (i) supplied sucrose affects the C/N and C/S ratios directly in shmt1 c-pgdh1 by increasing the C content, (ii) the further reduction in Rubisco oxygenase activity in shmt1 c-pgdh1 affects the N and S status, or (iii) a combination of both factors. In line with this hypothesis, the combination of PPSB and SHMT1 mutant backgrounds compensated for the imbalance in C, N, and S levels and modified the shoot/root developmental pattern by stimulating root versus shoot growth (Fig. 8).

The interaction between metabolism and development in plants is poorly understood. Our work provides important clues about how Gly/Ser fluxes modulate N/C and S/C ratios and shape plant developmental patterns in response to nutrient status. We show that PPSB is necessary for correct N and S partitioning between shoots and roots. Disrupting PPSB led to an imbalance in this partitioning, leading to an N and S deficit in shoots and a general response to nutrient deficiency. Forcing the exit of Gly out of the photorespiratory cycle by inhibiting SHMT1 led to changes in folate, SAM, and Asp metabolism that reversed the changes in N and S deficiency in shoots of the PPSB-deficient lines. Therefore, the regulation of the Ser-Gly-1C network is crucial for N, C, and S homeostasis. Several hypotheses have been put forward to explain the role of photorespiration in N and S metabolism. Our results provide genetic and biochemical evidence that the regulation of the SHMT1/GDC activity ratio is a key target linking photorespiration to N and S metabolism at the metabolic and transcriptional levels. Therefore, both the photorespiratory and PPSB pathways modulate N, S, and C fluxes through the Ser-Gly-1C network. In mammals, this network is considered to be a central integrator of nutrient status (Locasale 2013). We propose a similar role for the Ser-Gly-1C network for plants. Genetic engineering of SHMT/GDC and PGDH activity is expected to be a useful target to improve the N and S contents of crops under forthcoming climate change conditions. To validate the viability of this biotechnological approach, additional experiments will need to be conducted in natural environments under varying temperature, light, and CO2 conditions.

#### Materials and methods

#### Plant material and growth conditions

Original Arabidopsis (A. thaliana) seed stocks (ecotype Columbia-0 or Landsberg erecta) were supplied by the

European Arabidopsis Stock Center (Scholl et al. 2000). Conditional mutants with reduced expression of PSP1 (c-psp1.1 and c-psp1.2) and PGDH1 (c-pgdh1.1 and c-pgdh1.2) were obtained as previously described (Cascales-Miñana et al. 2013; Casatejada-Anchel et al. 2021). The shmt1.2 mutant (Voll et al. 2006) was kindly supplied by Prof Hermann Bauwe (Rostok, Germany). The mutant alleles of At5g26780 (shmt2.2; SALK 096265) and At2g13360 (sgat1; GT\_5\_6208) were selected in the SIGnAL Collection database at the Salk Institute (Alonso et al. 2003) and were identified by PCR genotyping with the primers listed in Supplemental Table S2. PPSB-deficient double mutants with shmt1.2 and shmt2.2 (shmt1.2 c-psp1.1, shmt1.2 c-psp1.2, shmt1.2 c-pgdh1.1, shmt1.2 c-pgdh1.2, shmt2.2 c-psp1.1, shmt2.2 c-psp1.2, shmt2.2 c-pgdh1.1, and shmt2.2 c-pgdh1.2) were generated by crossing single shmt1.2 and shmt2.2 mutants with PPSB-deficient mutants and identified by PCR genotyping with the primers listed in Supplemental Table S2.

Unless otherwise stated, seeds were sterilized and sown on 0.8% agar plates containing 1/5 strength MS medium with Gamborg vitamins buffered with 0.9 g L<sup>-1</sup> MES, adjusted to pH 5.7 with Tris (1/5 MS). After 2 to 4 d of stratification at 4 °C, the plates were vertically placed at 22 °C under a 16-h day/8-h night photoperiod at 100  $\mu$ mol m<sup>-2</sup> s<sup>-1</sup> light intensity (Lumilux fluorescent cool white, OSRAM EAN 4050300517797) and under aCO<sub>2</sub> or eCO<sub>2</sub> (2000 ppm) conditions for 14 to 16 d before sampling the seedlings. When indicated, 2% sucrose was added to the growth medium.

#### **Grafting experiments**

To graft the double mutant shmt1.2 c-psp1 shoot (scion) with the PPSB-deficient c-psp1 root (root-stock) and for selfgrafting of PPSB-deficient c-psp1, the protocol described by Thieme et al. (2015) was followed with some modifications. In short, plants were grown vertically on solid 1/5 MS medium containing 1.5% (w/v) agar at 22 °C and 2,000 ppm of CO2 under a 16-h day/8-h night photoperiod and 100  $\mu$ mol m<sup>-2</sup> s<sup>-1</sup> light. One day before grafting, plates containing the seedlings were covered with aluminum foil to favor the elongation of the mutant's hypocotyls. Seven to eight days after germination, evenly elongated hypocotyls were cut transversely in the upper half of the hypocotyl with a sterile razor blade, and the scions were combined with the root stock. Graft junctions were supported using a silicon tube with a 0.51 mm internal diameter, and grafted plants were transferred onto new sterile plates with 1/2 MS containing 1.5% (w/v) agar and grown under the same conditions as mentioned above. Every 3 d, the formation of adventitious roots originating from the scion was checked and whenever possible carefully removed.

#### Metabolite determination

Shoots and roots of 15-d-old plants grown on vertical plates were used to determine metabolite content in derivatized methanol extracts by gas chromatography-MS (GC-MS) as described by Lisec et al. (2006). Plants were sampled after

10-h of growth in the light. Folates were analyzed according to Wu et al. (2018). SAM analysis was performed as previously described (Hung et al. 2013). For adenosine measurements, 100 mg (fresh weight) of tissue was resuspended in 100  $\mu$ L of HClO<sub>4</sub> 1 m. After a 10-min centrifugation at 11,500 rpm at 4 °C, the supernatant was analyzed by LC-MS-MS as described by Fung et al. (2001).

#### 15N enrichment of the metabolome

Seeds were surface sterilized and sown on 1/5 MS plates containing 0.8% agar and kept in the dark at 4 °C for 4 d to synchronize germination. The plates were then incubated at 22 °C under a 16-h day/8-h night photoperiod at a light level of 100  $\mu$ mol m<sup>-2</sup> s<sup>-1</sup> and eCO<sub>2</sub> in a phytotron chamber. After 5 d of germination, the seedlings were transferred to hydroponic cultures as previously described (Erban et al. 2020). Briefly, seedlings were grown for 12 d in sterile glass containers with a metal net for support and liquid 1/5 MS medium. After reaching the morphological stage of 1.05 (Boyes et al. 2001), plants were transferred to new hydroponic medium containing 0.8 mm ammonium nitrate as the sole nitrogen source labeled or unlabeled with the stable isotope <sup>15</sup>N, <sup>15</sup>NH<sub>4</sub><sup>15</sup>NO<sub>3</sub> (Sigma-Aldrich, Ref. 366528), or <sup>14</sup>NH<sub>4</sub> <sup>14</sup>NO<sub>3</sub> (Sigma-Aldrich, Ref. 221244). After 3 d, shoots and roots were harvested separately and immediately frozen. The roots from the labeled media were washed with unlabeled 1/5 MS medium to detach the labeled ions. Extraction of metabolites was performed as described by Erban et al. (2020) and analyzed by GC-MS.

The raw chromatograms were baseline corrected and deconvoluted in ChromaTOF. Subsequently, the files were exported as .netCDF files. The .netCDF files were imported into TagFinder (Luedemann et al. 2008), setting the intensity threshold for upload into TagFinder to one, so as to include low abundance peaks such as multiply 15N-labeled isotopologs. Internal retention time standards of n-alkanes C<sub>10</sub> to C<sub>36</sub> (decane, dodecane, pentadecane, octadecane, nonadecane, docosane, octacosane, dotriacontane, hexatriacontane) were used to align the chromatograms. Peak intensities were scaled to the maximum of all peaks with the same m/z ratio and retention index window set to 0.05. Compounds were identified using the Golm Metabolome Database (Hummel et al. 2007). Due to isotopic envelope shifts, N-containing metabolites were manually annotated. <sup>13</sup>C<sub>6</sub>-Sorbitol was used as the internal standard of the polar phase. The normalization factor applied to each sample was the product of the fresh weight per sample multiplied by the intensity of the internal standard. Annotated mass features from the Golm Metabolome Database were used as targets for <sup>15</sup>N isotopic tracing analysis of each N-containing metabolite. In particular, mass features that contained one or more N atoms in their molecular formulas were used. The natural isotopic abundance (NIA) of mass features was corrected for across all detected isotopologs. The sum of the corrected <sup>15</sup>N-labeled isotopolog intensities divided by the total <sup>14</sup>Nand <sup>15</sup>N-pool was considered to be the mean fractional enrichment. All calculations were performed as previously described (Huege et al. 2014; Heinrich et al. 2018; Millard et al. 2019). The <sup>15</sup>N relative abundance reflects the relative amount of the metabolite pool that was newly synthesized since it incorporated the <sup>15</sup>N during our experiment. The nominal values were considered to be the sum of all detected isotopologs per mass feature after correcting NIA. In cases where one isotopolog was used for correction, the <sup>15</sup>N relative abundance is the NIA-corrected abundance of the first isotopolog.

## Elemental analyses, nitrate, and ammonium quantification

NH<sub>4</sub><sup>+</sup> analysis was performed using the Berthelot method as described by Weatherburn (1967). NO<sub>3</sub><sup>-</sup> was determined as described by Zhao and Wang (2017). Elemental analysis was performed using the Pregl-Dumas method with a CHNS elemental analyzer (Thermofisher SmartFlash model).

#### Gene expression analyses and RNA-seq

Reverse transcription quantitative PCR analysis was performed as described recently (Casatejada-Anchel et al. 2021). The primers used are listed in Supplemental Table S2. For RNA-seq, shoots and roots of 14-d-old plants vertically grown on 1/5 MS plates under eCO2 conditions were used. Three independent biological replicates of each sample were harvested after the 10-h light period for analysis. Total RNA extraction, RNA-seq library preparation, and sequencing were performed as previously described (Anoman et al. 2019). Quality check, trimming, alignment, reads counting, and filtering of genes expressed at low levels were conducted as previously described (Sun et al. 2018). PCA was performed on the TMM-normalized gene matrix after removing genes that are not expressed using the R function prcomp. Filtered genes were used to perform differential gene expression analysis with EdgeR. Genes were considered to be significantly differentially expressed if the corrected P-value (false discovery rate, FDR) was <0.05. Gene Ontology Enrichment Analysis was performed in agriGO v2.0 (Tian et al. 2017) based on a hypergeometric test.

#### Analysis of glutamine synthetase activity

GS activity was determined from crude extracts using the biosynthetic enzyme assay as previously described by Márquez et al. (2005). Crude extracts were obtained as described by García-Calderón et al. (2012). Shoots and roots were harvested from 14-d-old plants grown under eCO<sub>2</sub> conditions on 1/5 MS plates.

# Analysis of protein biosynthesis using <sup>35</sup>S-labeled Met/Cys and analysis of total protein content

The analysis of tracer incorporation into proteins using a <sup>35</sup>S-labeled L-Met/L-Cys cocktail (NEG77200MC) was performed as described previously (Zimmermann et al. 2021). Plant material was incubated in hydroponic culture

containing 1/5 MS medium supplemented with 0.1 mm Met traced by 6.3  $\mu$ Ci  $^{35}$ S-labeled L-Met/L-Cys cocktail per well for 6-h before harvesting. Total protein content was quantified with Bradford reagent (Bio-Rad) using bovine serum albumin as a standard.

#### Statistical analysis

Experimental values represent mean values and SE; *n* represents the number of independent samples. Significant differences compared with either the WT or control treatment were analyzed by Student's *t*-test algorithms (2-tailed) embedded in Microsoft Excel. Significant differences between groups were analyzed by 1-way ANOVA followed by Fisher's LSD test using IBM SPSS Statistics software. Bar plots were generated in GraphPad 8 software. The details of statistical analysis results are listed in Supplemental Data Sets 1 and 2.

#### **Accession numbers**

The original RNA-seq data were submitted to SRA under BioProject accession number PRJNA911249 (released 2023-10-11). The Arabidopsis locus identifiers for genes used in this study are as follows: *PSP1* (At1g18640), *PGDH1* (At4g34200), *SGAT* (At2g13360), *SHMT1* (At4g37930), and *SHMT2* (At5g26780).

#### Acknowledgments

The research of the R.R. group was supported by grant PID2019-107174GB-I00 funded by MCIN/AEI/10.13039/ 501100011033 and grant AICO/2021/300 funded by the Generalitat Valenciana. The research of S.K. was supported by the Deutsche Forschungsgemeinschaft (grant Kr4245/ 1-1; Kr4245/2-1). A.A.-E., R.C.-A., and S.R.-T. were supported by University of Valencia (Atracció de talent fellowship UV-INV\_PREDOC-1337025), the MCIN (FPI fellowship BES-2016-077943), and Generalitat Valenciana (APOSTD/ 2017/118), respectively. The research of the S.R. group was supported by grant NSF MCB-2015828. The authors would like to thank Prof. Hermann Bauwe for the generous gift of seeds of the shmt1.2 mutant used in this study. We also thank Dr. Friedrich Kragler for his support in the grafting experiment. Special thanks to Dr. Eleftheria Saplaoura, Dr. Eleni Mavrothalassiti, and Dr. Yin Xu for the technical assistance provided.

#### **Author contributions**

S.R.-T., A.A.-E., R.C.-A., J.M.-B., and S.K. participated in investigation and methodology. S.R.-T. and A.A.-E. participated in data analysis. TM and S.R.-T. participated in RNA-seq analysis and data curation. J.M.-B. and P.A. participated in protein biosynthesis experiments. S.S. and C.L.B. participated in folate analysis under the supervision of S.R. D.B.-M., S.R.-T., A.E., and F.M.-S. supported GC-MS data processing, i.e. TagFinder processing, metabolite and mass feature annotation, natural isotopic abundance correction, and statistical analyses under

the supervision of J.K. and A.R.F. S.R.-T., R.R., and A.R.F. conceived and designed the research. R.R., S.R., and S.R.-T. participated in conceptualization of the work. R.R. wrote the manuscript. A.R.F., S.R., S.K., J.K., P.A., J.M.-B., and S.R.-T. revised the manuscript. R.R. and A.R.F. supervised the work and provided funding.

#### Supplemental data

The following materials are available in the online version of this article.

**Supplemental Figure S1.** Amino acid levels in *sgat* mutant and WT shoots under aCO<sub>2</sub> and eCO<sub>2</sub> conditions.

**Supplemental Figure S2.** Glycolate levels in shoots of PPSB-deficient and PPSB-SHMT1-deficient lines.

**Supplemental Figure S3.** Heat map showing variation in metabolite levels when plants were shifted from eCO<sub>2</sub> to aCO<sub>2</sub> growth conditions.

**Supplemental Figure S4.** Grafting of scion *shmt1.2 c-psp1* shoots into *c-psp1* roots.

**Supplemental Figure S5.** Phenotypic characterization of *shmt2* mutants.

Supplemental Figure S6. PCA of RNA-seq data.

**Supplemental Figure S7.** Differential gene expression in the pyrimidine metabolic pathway in PPSB-deficient lines versus WT and SHMT-deficient lines versus *c-pgdh1* lines.

**Supplemental Figure S8.** NH<sub>4</sub><sup>+</sup> content in shoots and roots of different lines grown under eCO<sub>2</sub> conditions.

**Supplemental Table S1.** Carbon (C), nitrogen (N), and sulfur (S) content (mg/g dry weight) in shoots of WT and PPSB-deficient (*c-pgdh1*) lines growth under aCO<sub>2</sub> conditions.

**Supplemental Table S2.** List of primers used in this work. **Supplemental Data Set 1.** Statistical analysis of results in Tables and Figures.

**Supplemental Data Set 2.** Statistical analysis of results in Supplemental Tables and Supplemental Figures.

Conflict of interest statement. None declared.

#### Data availability

The materials generated in this work are available on reasonable request to the authors.

#### References

Abadie C, Boex-Fontvieille ERA, Carroll AJ, Tcherkez G. In vivo stoichiometry of photorespiratory metabolism. Nat Plants. 2016:2(2): 15220. https://doi.org/10.1038/nplants.2015.220

**Abadie C, Tcherkez G**. Plant sulphur metabolism is stimulated by photorespiration. Commun Biol. 2019:**2**(1):379. https://doi.org/10. 1038/s42003-019-0616-y

**Ainsworth EA, Long SP.** 30 Years of free-air carbon dioxide enrichment (FACE): what have we learned about future crop productivity and its potential for adaptation? Glob Chang Biol. 2020:**27**(1):27–49. https://doi.org/10.1111/gcb.15375

Alonso JM, Stepanova AN, Leisse TJ, Kim CJ, Chen H, Shinn P, Stevenson DK, Zimmerman J, Barajas P, Cheuk R, et al. Genome-wide insertional mutagenesis of Arabidopsis thaliana.

- Science. 2003:**301**(5633):653–657. https://doi.org/10.1126/science. 1086391
- Andrews M, Condron LM, Kemp PD, Topping JF, Lindsey K, Hodge S, Raven JA. Will rising atmospheric CO<sub>2</sub> concentration inhibit nitrate assimilation in shoots but enhance it in roots of C3 plants? Physiol Plant. 2020:**170**(1):40–45. https://doi.org/10.1111/ppl.13096
- Anoman AD, Flores-Tornero M, Benstein RM, Blau S, Rosa-Téllez S, Bräutigam A, Fernie AR, Muñoz-Bertomeu J, Schilasky S, Meyer AJ, et al. Deficiency in the phosphorylated pathway of serine biosynthesis perturbs sulfur assimilation. Plant Physiol. 2019:180(1): 153–170. https://doi.org/10.1104/pp.18.01549
- Baslam M, Mitsui T, Hodges M, Priesack E, Herritt MT, Aranjuelo I, Sanz-Sáez Á. Photosynthesis in a changing global climate: scaling up and scaling down in crops. Front Plant Sci. 2020:11:882. https://doi.org/10.3389/fpls.2020.00882
- Bauwe H, Hagemann M, Fernie AR. Photorespiration: players, partners and origin. Trends Plant Sci. 2010:15(6):330–336. https://doi.org/10.1016/j.tplants.2010.03.006
- **Bauwe H, Kolukisaoglu U**. Genetic manipulation of glycine decarboxylation. J Exp Bot. 2003:**54**(387):1523–1535. https://doi.org/10.1093/jxb/erg171
- Benstein RM, Ludewig K, Wulfert S, Wittek S, Gigolashvili T, Frerigmann H, Gierth M, Flügge UI, Krueger S. Arabidopsis phosphoglycerate dehydrogenase1 of the phosphoserine pathway is essential for development and required for ammonium assimilation and tryptophan biosynthesis. Plant Cell. 2013:25(12):5011–5029. https://doi.org/10.1105/tpc.113.118992
- Betti M, Bauwe H, Busch FA, Fernie AR, Keech O, Levey M, Ort DR, Parry MAJ, Sage R, Timm S, et al. Manipulating photorespiration to increase plant productivity: recent advances and perspectives for crop improvement. J Exp Bot. 2016:67(10):2977–2988. https://doi.org/10.1093/jxb/erw076
- **Bloom AJ.** Photorespiration and nitrate assimilation: a major intersection between plant carbon and nitrogen. Photosynth Res. 2015:**123**(2):117–128. https://doi.org/10.1007/s11120-014-0056-y
- **Bloom AJ, Asensio JSR, Randall L, Rachmilevitch S, Cousins AB, Carlisle EA**. CO<sub>2</sub> Enrichment inhibits shoot nitrate assimilation in C<sub>3</sub> but not C<sub>4</sub> plants and slows growth under nitrate in C<sub>3</sub> plants. Ecology. 2012:**93**(2):355–367. https://doi.org/10.1890/11-0485.1
- Bloom AJ, Burger M, Asensio JSR, Cousins AB. Carbon dioxide enrichment inhibits nitrate assimilation in wheat and Arabidopsis. Science. 2010:328(5980):899–903. https://doi.org/10.1126/science. 1186440
- **Bloom AJ, Burger M, Kimball BA, Pinter PJ.** Nitrate assimilation is inhibited by elevated CO<sub>2</sub> in field-grown wheat. Nat Clim Chang. 2014:**4**(6):477–480. https://doi.org/10.1038/nclimate2183
- **Bloom AJ, Kasemsap P, Rubio-Asensio JS**. Rising atmospheric CO<sub>2</sub> concentration inhibits nitrate assimilation in shoots but enhances it in roots of C<sub>3</sub> plants. Physiol Plant. 2020:**168**(4):963–972. https://doi.org/10.1111/ppl.13040
- **Bloom AJ, Lancaster KM**. Manganese binding to Rubisco could drive a photorespiratory pathway that increases the energy efficiency of photosynthesis. Nat Plants. 2018:**4**(7):414–422. https://doi.org/10.1038/s41477-018-0191-0
- Bonas U, Schmitz K, Rennenberg H, Bergmann L. Phloem transport of sulfur in *Ricinus*. Planta. 1982:**155**(1):82–88. https://doi.org/10.1007/ BF00402936
- Boyes DC, Zayed AM, Ascenzi R, McCaskill AJ, Hoffman NE, Davis KR, Görlach J. Growth stage-based phenotypic analysis of Arabidopsis: a model for high throughput functional genomics in plants. Plant Cell. 2001:13(7):1499–1510. https://doi.org/10.1105/tpc.010011
- **Busch FA, Sage RF, Farquhar GD**. Plants increase CO<sub>2</sub> uptake by assimilating nitrogen via the photorespiratory pathway. Nat Plants. 2018:**4**(1):46–54. https://doi.org/10.1038/s41477-017-0065-x
- Cao M-J, Wang Z, Wirtz M, Hell R, Oliver DJ, Xiang C-B. SULTR3; 1 is a chloroplast-localized sulfate transporter in *Arabidopsis thaliana*. Plant J. 2013:**73**(4):607–616. https://doi.org/10.1111/tpj.12059

- Casatejada-Anchel R, Muñoz-Bertomeu J, Rosa-Téllez S, Anoman AD, Nebauer SG, Torres-Moncho A, Fernie AR, Ros R. Phosphoglycerate dehydrogenase genes differentially affect Arabidopsis metabolism and development. Plant Sci. 2021:306: 110863. https://doi.org/10.1016/j.plantsci.2021.110863
- Cascales-Miñana B, Muñoz-Bertomeu J, Flores-Tornero M, Anoman AD, Pertusa J, Alaiz M, Osorio S, Fernie AR, Segura J, Ros R. The phosphorylated pathway of serine biosynthesis is essential both for male gametophyte and embryo development and for root growth in *Arabidopsis*. Plant Cell. 2013:25(6):2084–2101. https://doi.org/10.1105/tpc.113.112359
- Cotton CA, Edlich-Muth C, Bar-Even A. Reinforcing carbon fixation: CO<sub>2</sub> reduction replacing and supporting carboxylation. Curr Opin Biotechnol. 2018:**49**:49–56. https://doi.org/10.1016/j.copbio.2017.07. 014
- Davidian JC, Kopriva S. Regulation of sulfate uptake and assimilation—the same or not the same? Mol Plant. 2010:3(2):314–325. https://doi.org/10.1093/mp/ssq001
- **Douce R, Bourguignon J, Neuburger M, Rebeille F.** The glycine decarboxylase system: a fascinating complex. Trends Plant Sci. 2001:**6**(4):167–176. https://doi.org/10.1016/S1360-1385(01)01892-1
- **Ducker GS, Rabinowitz JD.** One-carbon metabolism in health and disease. Cell Metab. 2017:**25**(1):27–42. https://doi.org/10.1016/j.cmet. 2016.08.009
- Eisenhut M, Bräutigam A, Timm S, Florian A, Tohge T, Fernie AR, Bauwe H, Weber APM. Photorespiration is crucial for dynamic response of photosynthetic metabolism and stomatal movement to altered CO<sub>2</sub> availability. Mol Plant. 2017:10(1):47–61. https://doi.org/10.1016/j.molp.2016.09.011
- **Eisenhut M, Roell MS, Weber APM**. Mechanistic understanding of photorespiration paves the way to a new green revolution. New Phytologist. 2019:**223**(4):1762–1769. https://doi.org/10.1111/nph. 15872
- Engel N, Ewald R, Gupta KJ, Zrenner R, Hagemann M, Bauwe H. The presequence of Arabidopsis serine hydroxymethyltransferase SHM2 selectively prevents import into mesophyll mitochondria. Plant Physiol. 2011:157(4):1711–1720. https://doi.org/10.1104/pp.111.184564
- Engel N, van den Daele K, Kolukisaoglu U, Morgenthal K, Weckwerth W, Parnik T, Keerberg O, Bauwe H. Deletion of glycine decarboxylase in Arabidopsis is lethal under nonphotorespiratory conditions. Plant Physiol. 2007:144(3):1328–1335. https://doi.org/10.1104/pp.107.099317
- Erban A, Martinez-Seidel F, Rajarathinam Y, Dethloff F, Orf I, Fehrle I, Alpers J, Beine-Golovchuk O, Kopka J. Multiplexed profiling and data processing methods to identify temperature-regulated primary metabolites using gas chromatography coupled to mass spectrometry. Methods Mol Biol. 2020:2156:203–239. https://doi.org/10.1007/978-1-0716-0660-5\_15
- Fernie AR, Bauwe H. Wasteful, essential, evolutionary stepping stone? The multiple personalities of the photorespiratory pathway. Plant J. 2020:102(4):666–677. https://doi.org/10.1111/tpj.14669
- Flügel F, Timm S, Arrivault S, Florian A, Stitt M, Fernie AR, Bauwe H. The photorespiratory metabolite 2-phosphoglycolate regulates photosynthesis and starch accumulation in *Arabidopsis*. Plant Cell. 2017;**29**(10):2537–2551. https://doi.org/10.1105/tpc.17.00256
- **Fu X, Gegory LM, Weise SE, Walker BJ**. Integrated flux and pool size analysis in plant central metabolism reveals unique roles of glycine and serine during photorespiration. Nat Plants. 2023:9(1):169–178. https://doi.org/10.1038/s41477-022-01294-9
- **Fung EN, Cai Z, Burnette TC, Sinhababu AK.** Simultaneous determination of Ziagen and its phosphorylated metabolites by ion-pairing high-performance liquid chromatography-tandem mass spectrometry. J Chromatogr B Biomed Sci Appl. 2001:**754**(2):285–295. https://doi.org/10.1016/S0378-4347(00)00619-8
- Galili G, Amir R, Fernie AR. The regulation of essential amino acid synthesis and accumulation in plants. Annu Rev Plant Biol. 2016:67(1): 153–178. https://doi.org/10.1146/annurev-arplant-043015-112213

- García-Calderón M, Chiurazzi M, Espuny MR, Márquez AJ. Photorespiratory metabolism and nodule function: behavior of *Lotus japonicus* mutants deficient in plastid glutamine synthetase. Mol Plant-Microbe Interac. 2012:25(2):211–219. https://doi.org/10.1094/MPMI-07-11-0200
- Geeraerts SL, Heylen E, de Keersmaecker K, Kampen KR. The ins and outs of serine and glycine metabolism in cancer. Nat Metab. 2021:3(2):131–141. https://doi.org/10.1038/s42255-020-00329-9
- Gorelova V, Ambach L, Rébeillé F, Stove C, Van Der Straeten D. Folates in plants: research advances and progress in crop biofortification. Front Chem. 2017:**5**:21. https://doi.org/10.3389/fchem.2017.00021
- Hanson AD, Gregory JF 3rd. Folate biosynthesis, turnover, transport in plants. Annu Rev Plant Biol. 2011:62(1):105–125. https://doi.org/10.1146/annurev-arplant-042110-103819
- Heinrich P, Kohler C, Ellmann L, Kuerner P, Spang R, Oefner PJ, Dettmer K. Correcting for natural isotope abundance and tracer impurity in MS-, MS/MS- and high-resolution-multiple-tracer-data from stable isotope labeling experiments with IsoCorrectoR. Sci Rep. 2018:8(1):17910. https://doi.org/10.1038/s41598-018-36293-4
- **Ho CL, Saito K**. Molecular biology of the plastidic phosphorylated serine biosynthetic pathway in *Arabidopsis thaliana*. Amino Acids. 2001:**20**(3):243–259. https://doi.org/10.1007/s007260170042
- Huege J, Goetze J, Dethloff F, Junker B, Kopka J. Quantification of stable isotope label in metabolites via mass spectrometry. Methods Mol Biol. 2014:1056:213–223. https://doi.org/10.1007/978-1-62703-592-7 20
- **Hummel J, Selbig J, Walther D, Kopka J**. The Golm Metabolome Database: a database for GC-MS based metabolite profiling BT-metabolomics: a powerful tool in systems biology. In: **Nielsen J, Jewett MC**, editors. Berlin, Heidelberg: Springer Berlin Heidelberg; 2007. p. 75–95.
- Hung CY, Fan L, Kittur FS, Sun K, Qiu J, Tang S, Holliday BM, Xiao B, Burkey KO, Bush LP, et al. Alteration of the alkaloid profile in genetically modified tobacco reveals a role of methylenetetrahydrofolate reductase in nicotine N-demethylation. Plant Physiol. 2013:161(2): 1049–1060. https://doi.org/10.1104/pp.112.209247
- Jauregui I, Aparicio-Tejo PM, Avila C, Cañas R, Sakalauskiene S, Aranjuelo I. Root-shoot interactions explain the reduction of leaf mineral content in Arabidopsis plants grown under elevated [CO<sub>2</sub>] conditions. Physiol Plant. 2016:158(1):65-79. https://doi.org/10. 1111/ppl.12417
- Jauregui I, Aroca R, Garnica M, Zamarreño ÁM, García-Mina JM, Serret MD, Parry M, Irigoyen JJ, Aranjuelo I. Nitrogen assimilation and transpiration: key processes conditioning responsiveness of wheat to elevated [CO<sub>2</sub>] and temperature. Physiol Plan t. 2015:158(3):338–354. https://doi.org/10.1111/ppl.12345
- Jiang L, Liu Y, Sun H, Han Y, Li J, Li C, Guo W, Meng H, Li S, Fan Y, et al. The mitochondrial folylpolyglutamate synthetase gene is required for nitrogen utilization during early seedling development in Arabidopsis. Plant Physiol. 2013:161(2):971–989. https://doi.org/10.1104/pp.112.203430
- Kebeish R, Niessen M, Thiruveedhi K, Bari R, Hirsch HJ, Rosenkranz R, Stabler N, Schonfeld B, Kreuzaler F, Peterhansel C. Chloroplastic photorespiratory bypass increases photosynthesis and biomass production in *Arabidopsis thaliana*. Nat Biotechnol. 2007:25(5): 593–599. https://doi.org/10.1038/nbt1299
- **Kleczkowski LA, Givan CV**. Serine formation in leaves by mechanisms other than the glycolate pathway. J Plant Physiol. 1988:**132**(6): 641–652. https://doi.org/10.1016/S0176-1617(88)80223-2
- **Krämer K, Kepp G, Brock J, Stutz S, Heyer AG**. Acclimation to elevated CO<sub>2</sub> affects the C/N balance by reducing de novo N-assimilation. Physiol Plant. 2022:**174**(1):e13615. https://doi.org/10.1111/ppl.13615
- Lappartient AG, Vidmar JJ, Leustek T, Glass ADM, Touraine B. Inter-organ signaling in plants: regulation of ATP sulfurylase and sulfate transporter genes expression in roots mediated by phloem-

- translocated compound. Plant J. 1999:**18**(1):89–95. https://doi.org/10.1046/j.1365-313X.1999.00416.x
- Li W, Liang Q, Mishra RC, Sanchez-Muñoz R, Wang H, Chen X, van der Straeten D, Zhang C, Xiao Y. The 5-formyl-tetrahydrofolate proteome links folates with C/N metabolism and reveals feedback regulation of folate biosynthesis. Plant Cell. 2021:33(10):3367–3385. https://doi.org/10.1093/plcell/koab198
- Lisec J, Schauer N, Kopka J, Willmitzer L, Fernie AR. Gas chromatography mass spectrometry–based metabolite profiling in plants. Nat Protoc. 2006:1(1):387–396. https://doi.org/10.1038/nprot.2006.59
- Lobo AK, de Oliveira Martins M, Lima Neto MC, Machado EC, Ribeiro RV, Silveira JA. Exogenous sucrose supply changes sugar metabolism and reduces photosynthesis of sugarcane through the down-regulation of Rubisco abundance and activity. J Plant Physiol. 2015:179:113–121. https://doi.org/10.1016/j.jplph.2015.03.007
- Locasale JW. Serine, glycine and one-carbon units: cancer metabolism in full circle. Nat Rev Cancer. 2013:13(8):572–583. https://doi.org/10.1038/nrc3557
- Locasale JW, Grassian AR, Melman T, Lyssiotis CA, Mattaini KR, Bass AJ, Heffron G, Metallo CM, Muranen T, Sharfi H, et al. Phosphoglycerate dehydrogenase diverts glycolytic flux and contributes to oncogenesis. Nat Genet. 2011:43(9):869–874. https://doi.org/10.1038/ng.890
- **Luedemann A, Strassburg K, Erban A, Kopka J.** Tagfinder for the quantitative analysis of gas chromatography–mass spectrometry (GC-MS)-based metabolite profiling experiments. Bioinformatics. 2008:**24**(5):732–737. https://doi.org/10.1093/bioinformatics/btn023
- Maeda Y, Konishi M, Kiba T, Sakuraba Y, Sawaki N, Kurai T, Ueda Y, Sakakibara H, Yanagisawa S. A NIGT1-centred transcriptional cascade regulates nitrate signalling and incorporates phosphorus starvation signals in Arabidopsis. Nat Commun. 2018:9(1):1376. https://doi.org/10.1038/s41467-018-03832-6
- Márquez AJ, Betti M, García-Calderón M, Pal'ove-Balang P, Díaz P, Monza J. Nitrate assimilation in Lotus japonicus. J Exp Bot. 2005:56(417):1741–1749. https://doi.org/10.1093/jxb/eri171
- Medek DE, Schwartz J, Myers SS. Estimated effects of future atmospheric CO<sub>2</sub> concentrations on protein intake and the risk of protein deficiency by country and region. Environ Health Perspect. 2017:125(8):087002. https://doi.org/10.1289/EHP41
- Meng H, Jiang L, Xu B, Guo W, Li J, Zhu X, Qi X, Duan L, Meng X, Fan Y, et al. Arabidopsis plastidial folylpolyglutamate synthetase is required for seed reserve accumulation and seedling establishment in darkness. PLoS One. 2014:9(7):e101905. https://doi.org/10.1371/journal.pone.0101905
- Millard P, Delépine B, Guionnet M, Heuillet M, Bellvert F, Létisse F. Isocor: isotope correction for high-resolution MS labeling experiments. Bioinformatics. 2019:35(21):4484–4487. https://doi.org/10.1093/bioinformatics/btz209
- Modde K, Timm S, Florian A, Michl K, Fernie AR, Bauwe H. High serine:glyoxylate aminotransferase activity lowers leaf daytime serine levels, inducing the phosphoserine pathway in Arabidopsis. J Exp Bot. 2017:68(3):643–656. https://doi.org/10.1093/jxb/erw467
- Mohanta TK, Khan AL, Hashem A, Abd-Allah EF, Yadav D, Al-Harrasi A. Genomic and evolutionary aspects of chloroplast tRNA in monocot plants. BMC Plant Biol. 2019:19(1):39. https://doi.org/10.1186/s12870-018-1625-6
- Mouillon JM, Aubert S, Bourguignon J, Gout E, Douce R, Rebeille F. Glycine and serine catabolism in non-photosynthetic higher plant cells: their role in C1 metabolism. Plant J. 1999:20(2):197–205. https://doi.org/10.1046/j.1365-313x.1999.00591.x
- Myers SS, Zanobetti A, Kloog I, Huybers P, Leakey ADB, Bloom AJ, Carlisle E, Dietterich LH, Fitzgerald G, Hasegawa T, et al. Increasing CO<sub>2</sub> threatens human nutrition. Nature. 2014: **510**(7503):139–142. https://doi.org/10.1038/nature13179
- Novitskaya L, Trevanion SJ, Driscoll S, Foyer CH, Noctor G. How does photorespiration modulate leaf amino acid contents? A dual approach through modelling and metabolite analysis. Plant Cell

- Environ. 2002:**25**(7):821–835. https://doi.org/10.1046/j.1365-3040.
- **Ogren WL**. Affixing the O to Rubisco: discovering the source of photorespiratory glycolate and its regulation. Photosynth Res. 2003: **76**(1/3):53–63. https://doi.org/10.1023/A:1024913925002
- **Ogren WL, Bowes G.** Ribulose diphosphate carboxylase regulates soybean photorespiration. Nat New Biol. 1971:**230**(13):159–160. https://doi.org/10.1038/newbio230159a0
- Pacold ME, Brimacombe KR, Chan SH, Rohde JM, Lewis CA, Swier LJYM, Possemato R, Chen WW, Sullivan LB, Fiske BP, et al. A PHGDH inhibitor reveals coordination of serine synthesis and one-carbon unit fate. Nat Chem Biol. 2016:12(6):452–458. https://doi.org/10.1038/nchembio.2070
- Peterhansel C, Horst I, Niessen M, Blume C, Kebeish R, Kurkcuoglu S, Kreuzaler F, Maurino V G, Horst I, Niessen M, et al. Photorespiration. Arabidopsis Book. 2010:8:e0130. https://doi.org/10.1199/tab.0130
- Possemato R, Marks KM, Shaul YD, Pacold ME, Kim D, Birsoy K, Sethumadhavan S, Woo HK, Jang HG, Jha AK, et al. Functional genomics reveal that the serine synthesis pathway is essential in breast cancer. Nature. 2011:476(7360):346-350. https://doi.org/10.1038/nature10350
- Quentin AG, Close DC, Hennen LMHP, Pinkard EA. Down-regulation of photosynthesis following girdling, but contrasting effects on fruit set and retention, in two sweet cherry cultivars. Plant Physiol Biochem. 2013:73:359–367. https://doi.org/10.1016/j.plaphy.2013.10.014
- Rachmilevitch S, Cousins AB, Bloom AJ. Nitrate assimilation in plant shoots depends on photorespiration. Proc Natl Acad Sci USA. 2004: 101(31):11506–11510. https://doi.org/10.1073/pnas.0404388101
- Ravanel S, Block MA, Rippert P, Jabrin S, Curien G, Rébeillé F, Douce R. Methionine metabolism in plants: chloroplasts are autonomous for de novo methionine synthesis and can import S-adenosylmethionine from the cytosol. J Biol Chem. 2004:279(21): 22548–22557. https://doi.org/10.1074/jbc.M313250200
- Rebeille F, Neuburger M, Douce R. Interaction between glycine decarboxylase, serine hydroxymethyltransferase and tetrahydrofolate polyglutamates in pea leaf mitochondria. Biochem J. 1994:302(1): 223–228. https://doi.org/10.1042/bj3020223
- Rébeillé F, Ravanel S, Jabrin S, Douce R, Storozhenko S, Van Der Straeten D. Folates in plants: biosynthesis, distribution, enhancement. Physiol Plant. 2006:126(3):330–342. https://doi.org/10.1111/j. 1399-3054.2006.00587.x
- Reina-Campos M, Diaz-Meco MT, Moscat J. The complexity of the serine glycine one-carbon pathway in cancer. J Cell Biol. 2019: 219(1):e201907022. https://doi.org/10.1083/jcb.201907022
- Rennenberg H, Schmitz K, Bergmann L. Long-distance transport of sulfur in Nicotiana tabacum. Planta. 1979:147(1):57–62. https://doi. org/10.1007/BF00384591
- **Ristova D, Kopriva S.** Sulfur signaling and starvation response in Arabidopsis. iScience. 2022:**25**(5):104242. https://doi.org/10.1016/j.isci.2022.104242
- Ritterhoff J, Young S, Villet O, Shao D, Neto FC, Bettcher LF, Hsu Y-WA, Kolwicz SC, Raftery D, Tian R. Metabolic remodeling promotes cardiac hypertrophy by directing glucose to aspartate biosynthesis. Circ Res. 2020:126(2):182–196. https://doi.org/10.1161/CIRCRESAHA.119.315483
- Ros R, Muñoz-Bertomeu J, Krueger S. Serine in plants: biosynthesis, metabolism, functions. Trends Plant Sci. 2014:19(9):564–569. https://doi.org/10.1016/j.tplants.2014.06.003
- Samuilov S, Brilhaus D, Rademacher N, Flachbart S, Arab L, Alfarraj S, Kuhnert F, Kopriva S, Weber APM, Mettler-Altmann T, et al. The photorespiratory BOU gene mutation alters sulfur assimilation and its crosstalk with carbon and nitrogen metabolism in Arabidopsis thaliana. Front Plant Sci. 2018a:9:1709. https://doi.org/10.3389/fpls.2018.01709
- Samuilov S, Rademacher N, Brilhaus D, Flachbart S, Arab L, Kopriva S, Weber APM, Mettler-Altmann T, Rennenberg H. Knock-down of the phosphoserine phosphatase gene effects rather N-Than

- S-metabolism in Arabidopsis thaliana. Front Plant Sci. 2018b:9: 1930. https://doi.org/10.3389/fpls.2018.01830
- Sauter M, Moffatt B, Saechao MC, Hell R, Wirtz M. Methionine salvage and S-adenosylmethionine: essential links between sulfur, ethylene and polyamine biosynthesis. Biochem J. 2013:451(2):145–154. https://doi.org/10.1042/BJ20121744
- Scholl RL, May ST, Ware DH. Seed and molecular resources for Arabidopsis. Plant Physiol. 2000:124(4):1477–1480. https://doi.org/10.1104/pp.124.4.1477
- Shen BR, Wang LM, Lin XL, Yao Z, Xu HW, Zhu CH, Teng HY, Cui LL, Liu EE, Zhang JJ, et al. Engineering a new chloroplastic photorespiratory bypass to increase photosynthetic efficiency and productivity in rice. Mol Plant. 2019:12(2):199–214. https://doi.org/10.1016/j.molp.2018.11.013
- **Shi X, Bloom A**. Photorespiration: the futile cycle? Plants. 2021:**10**(5): 908. https://doi.org/10.3390/plants10050908
- Somerville CR, Ogren WL. Photorespiration mutants of *Arabidopsis thaliana* deficient in serine-glyoxylate aminotransferase activity. Proc Natl Acad Sci USA. 1980:**77**(5):1711–1720. https://doi.org/10. 1073/pnas.77.5.2684
- **South PF, Cavanagh AP, Liu HW, Ort DR**. Synthetic glycolate metabolism pathways stimulate crop growth and productivity in the field. Science. 2019:**363**(6422):eaat9077. https://doi.org/10.1126/science. aat9077
- Stokes ME, Chattopadhyay A, Wilkins O, Nambara E, Campbell MM. Interplay between sucrose and folate modulates auxin signaling in Arabidopsis. Plant Physiol. 2013:162(3):1552–1565. https://doi.org/10.1104/pp.113.215095
- Sun X, Matus JT, Wong DCJ, Wang Z, Chai F, Zhang L, Fang T, Zhao L, Wang Y, Han Y, et al. The GARP/MYB-related grape transcription factor AQUILO improves cold tolerance and promotes the accumulation of raffinose family oligosaccharides. J Exp Bot. 2018:69(7): 1749–1764. https://doi.org/10.1093/jxb/ery020
- Tan Q, Zhang L, Grant J, Cooper P, Tegeder M. Increased phloem transport of S-methylmethionine positively affects sulfur and nitrogen metabolism and seed development in pea plants. Plant Physiol. 2010:154(4):1886–1896. https://doi.org/10.1104/pp.110.166389
- Thieme CJ, Rojas-Triana M, Stecyk E, Schudoma C, Zhang W, Yang L, Minambres M, Walther D, Schulze WX, Paz-Ares J, et al. Endogenous Arabidopsis messenger RNAs transported to distant tissues. Nat Plants. 2015:1(4):15025. https://doi.org/10.1038/nplants. 2015.25
- **Tian T, Liu Y, Yan H, You Q, Yi X, Du Z, Xu W, Su Z**. agriGO v2.0: a GO analysis toolkit for the agricultural community, 2017 update. Nucleic Acids Res. 2017:**45**(W1):W122–W129. https://doi.org/10.1093/nar/gkx382
- Timm S, Nunes-Nesi A, Florian A, Eisenhut M, Morgenthal K, Wirtz M, Hell R, Weckwerth W, Hagemann M, Fernie AR, et al. Metabolite profiling in *Arabidopsis thaliana* with moderately impaired photorespiration reveals novel metabolic links and compensatory mechanisms of photorespiration. Metabolites. 2021:11(6):391. https://doi.org/10.3390/metabo11060391
- **Tolbert NE**. The  $C_2$  oxidative photosynthetic carbon cycle. Annu Rev Plant Physiol Plant Mol Biol. 1997:**48**(1):1–25. https://doi.org/10. 1146/annurev.arplant.48.1.1
- Toujani W, Muñoz-Bertomeu J, Flores-Tornero M, Rosa-Tellez S, Anoman AD, Alseekh S, Fernie AR, Ros R. Functional characterization of the plastidial 3-phosphoglycerate dehydrogenase family in Arabidopsis. Plant Physiol. 2013:163(3):1164–1178. https://doi.org/10.1104/pp.113.226720
- Ueda Y, Kiba T, Yanagisawa S. Nitrate-inducible NIGT1 proteins modulate phosphate uptake and starvation signalling via transcriptional regulation of SPX genes. Plant J. 2020:102(3):448–466. https://doi.org/10.1111/tpj.14637
- **Voll LM, Jamai A, Renne P, Voll H, McClung CR, Weber AP**. The photorespiratory Arabidopsis *shm1* mutant is deficient in SHM1. Plant Physiol. 2006:**140**(1):59–66. https://doi.org/10.1104/pp.105. 071399

- Walker BJ, Vanloocke A, Bernacchi CJ, Ort DR. The costs of photorespiration to food production now and in the future. Annu Rev Plant Biol. 2016:67(1):107–129. https://doi.org/10.1146/annurevarplant-043015-111709
- **Watanabe M, Chiba Y, Hirai MY**. Metabolism and regulatory functions of O-acetylserine, S-adenosylmethionine, homocysteine, serine in plant development and environmental responses. Front Plant Sci. 2021:**12**:643403. https://doi.org/10.3389/fpls.2021.643403
- **Weatherburn MW**. Phenol-hypochlorite reaction for determination of ammonia. Anal Chem. 1967:**39**(8):971–974. https://doi.org/10.1021/ac60252a045
- Wieser H, Manderscheid R, Erbs M, Weigel H-J. Effects of elevated atmospheric CO<sub>2</sub> concentrations on the quantitative protein composition of wheat grain. J Agric Food Chem. 2008:**56**(15):6531–6535. https://doi.org/10.1021/jf8008603
- Witte CP, Herde M. Nucleotide metabolism in plants. Plant Physiol. 2020:182(1):63–78. https://doi.org/10.1104/pp.19.00955
- Wu Z, Ren H, Xiong W, Roje S, Liu Y, Su K, Fu C. Methylenetetrahydrofolate reductase modulates methyl metabolism and lignin monomer methylation in maize. J Exp Bot. 2018:69(16): 3963–3973. https://doi.org/10.1093/jxb/ery208

- Wulfert S, Krueger S. Phosphoserine aminotransferase1 is part of the phosphorylated pathways for serine biosynthesis and essential for light and sugar-dependent growth promotion. Front Plant Sci. 2018:9:1712. https://doi.org/10.3389/fpls.2018.01712
- Yang M, Vousden KH. Serine and one-carbon metabolism in cancer. Nat Rev Cancer. 2016:16(10):650–662. https://doi.org/10.1038/nrc.2016.81
- Yoshimoto N, Inoue E, Watanabe-Takahashi A, Saito K, Takahashi H. Posttranscriptional regulation of high-affinity sulfate transporters in Arabidopsis by sulfur nutrition. Plant Physiol. 2007:145(2): 378–388. https://doi.org/10.1104/pp.107.105742
- Zhao L, Wang Y. Nitrate assay for plant tissues. Bio Protoc. 2017:7(2): e2029. https://doi.org/10.21769/BioProtoc.2029
- Zimmermann SE, Benstein RM, Flores-Tornero M, Blau S, Anoman AD, Rosa-Téllez S, Gerlich SC, Salem MA, Alseekh S, Kopriva S, et al. The phosphorylated pathway of serine biosynthesis links plant growth with nitrogen metabolism. Plant Physiol. 2021:186(3): 1487–1506. https://doi.org/10.1093/plphys/kiab167
- Zrenner R, Riegler H, Marquard CR, Lange PR, Geserick C, Bartosz CE, Chen CT, Slocum RD. A functional analysis of the pyrimidine catabolic pathway in Arabidopsis. New Phytol. 2009:183(1): 117–132. https://doi.org/10.1111/j.1469-8137.2009.02843.x